

Pittsburg State University

## Pittsburg State University Digital Commons

---

Electronic Theses & Dissertations

Graduate School

---

Spring 5-15-2024

### STUDY OF SOYBEAN OIL-BASED NON-ISOCYANATE POLYURETHANE FILMS VIA A SOLVENT AND CATALYST-FREE APPROACH

Pratik Patel

Pittsburg State University, pratikpatel403040@gmail.com

Follow this and additional works at: <https://digitalcommons.pittstate.edu/etd>

---

#### Recommended Citation

Patel, Pratik, "STUDY OF SOYBEAN OIL-BASED NON-ISOCYANATE POLYURETHANE FILMS VIA A SOLVENT AND CATALYST-FREE APPROACH" (2024). *Electronic Theses & Dissertations*. 521.  
<https://digitalcommons.pittstate.edu/etd/521>

This Thesis is brought to you for free and open access by the Graduate School at Pittsburg State University Digital Commons. It has been accepted for inclusion in Electronic Theses & Dissertations by an authorized administrator of Pittsburg State University Digital Commons. For more information, please contact [digitalcommons@pittstate.edu](mailto:digitalcommons@pittstate.edu).

STUDY OF SOYBEAN OIL-BASED NON-ISOCYANATE POLYURETHANE FILMS  
VIA A SOLVENT AND CATALYST-FREE APPROACH

Thesis Submitted to the Graduate School  
in Partial Fulfilment of the Requirements  
For the Degree of  
Master of Science

Pratik Patel

Pittsburg State University

Pittsburg, Kansas

May 2024

STUDY OF SOYBEAN OIL-BASED NON-ISOCYANATE POLYURETHANE FILMS  
VIA A SOLVENT AND CATALYST-FREE APPROACH

Pratik Patel

APPROVED:

Thesis Advisor

\_\_\_\_\_  
Dr. Ram K. Gupta, Department of Chemistry

Committee Member

\_\_\_\_\_  
Dr. Khamis Siam, Department of Chemistry

Committee Member

\_\_\_\_\_  
Dr. Timothy Dawsey, National Institute for Materials Advancement

Committee Member

\_\_\_\_\_  
Dr. Anuradha Ghosh, Department of Biology

## Acknowledgments

I am immensely thankful to Dr. Ram K. Gupta, my supervisor extraordinaire, whose wisdom, unwavering support, and boundless creativity have been the wind beneath my academic wings. Dr. Gupta's guidance has been akin to navigating through a labyrinth with a seasoned guide, always leading me toward illuminating insights and innovative pathways. His commitment to excellence and penchant for pushing boundaries has transformed my research journey into a thrilling adventure. With heartfelt appreciation, I thank Dr. Gupta for his invaluable time, tireless dedication, and unwavering belief in my potential, which have been the catalysts for my academic growth and success.

I want to thank the faculty members, especially Dr. Khamis Siam, Dr. Tim Dawsey, and Dr. Anuradha Ghosh, for their constructive remarks and academic contributions, which significantly improved the quality of my thesis. Their faith in my ability has been the driving force behind my achievements. Special gratitude to my friends Niharika, Mayank, Rutu, Janvi, and Niyati for providing academic and moral support and fostering a positive and inspiring atmosphere where I could grow and develop.

I deeply thank my father, Mr. Shaileshbhai V. Patel, and my mother, Mrs. Ushaben S. Patel, whose unconditional love, and unwavering support have been the cornerstone of my journey. They have been my greatest source of inspiration, providing selfless love and guidance at every turn. Throughout my educational pursuit, my parents have stood by me, offering both emotional and financial support, for which I am profoundly grateful.

I'd also like to thank the Department of Chemistry and the National Institute for Materials Advancement at Pittsburg State University for their financial support, which

made this study possible. This thesis would not have been feasible without the collaborative efforts of these individuals and organizations. Thank you for being an important part of our educational endeavor.

# STUDY OF SOYBEAN OIL-BASED NON-ISOCYANATE POLYURETHANE FILMS VIA A SOLVENT AND CATALYST-FREE APPROACH

An Abstract of the Thesis by  
Pratik Patel

Synthesizing polymeric materials that are both sustainable and practical has become a priority. Polyurethanes (PU) are becoming more popular because of their countless applications and exclusive properties in many sectors. While considering the current issue of environmental problems and the excessive use of petroleum products, non-isocyanate polyurethanes (NIPU) are favored due to their sustainability and low toxicity compared to conventional PU. In this work, flexible NIPU films were made using a green and facile method. For that, soybean oil (SBO) was used as the starting material and converted into epoxide soybean oil (ESBO) followed by its chemical conversion into carbonated soybean oil (CSBO) using carbon dioxide (CO<sub>2</sub>) gas. Following that, the CSBO reacted with three different aliphatic amines, namely 1,2-ethylenediamine (EDA), 1,4-butylenediamine (BDA), and 1,6-hexamethylenediamine (HDA) in a solventless and catalyst-free system. The films were cast and cured at 85 °C at different curing times. The effects of the aliphatic diamines and curing times on the NIPU films were evaluated. The individual materials were confirmed with FT-IR, <sup>1</sup>H nuclear magnetic resonance, and gel permeation chromatography. To analyze the thermal and mechanical properties, thermogravimetric analysis, dynamic mechanical analysis, and differential scanning calorimetry were performed. Furthermore, mechanical tests such as hardness and tensile strength were also performed along with the degree of swelling, gel content, and contact angle using several solvents. This study elucidated the structure-property relationship based on the effect of

curing time and aliphatic chain size of diamines in the properties of a NIPU film. The satisfactory thermal and mechanical properties accompanied by a green and facile approach displayed the potential scalability of the NIPU films.

## Table of contents

<b>CHAPTER I.....</b>	<b>1</b>
<b>INTRODUCTION.....</b>	<b>1</b>
1.1. Background of Polyurethanes.....	1
1.2. Chemistry of Polyurethanes.....	2
1.3. Properties and Applications of Polyurethane Materials .....	3
1.3.1 PU Films.....	4
1.3.2. PU Adhesive and Coating.....	5
1.3.3. PU Foam.....	6
1.3.4. Elastomer.....	6
1.4. Drawbacks of Conventional Polyurethanes.....	7
1.5. Bio-based Polyurethane.....	7
1.6. Non-isocyanate Polyurethane.....	8
1.7. Research Objective.....	9
<b>CHAPTER II.....</b>	<b>11</b>
<b>MATERIALS AND METHODS.....</b>	<b>11</b>
2.1. Materials.....	11
2.1.1. Soybean Oil.....	11
2.1.2. Tetrabutylammonium Bromide.....	12
2.1.3. 1,2, Ethylene Diamine.....	12
2.1.4. 1,4-Butane Diamine.....	13
2.1.5. 1,6, Hexamethylene Diamine.....	13
2.1.6. Carbon Dioxide.....	14
2.2. Synthesis.....	14
2.2.1. Synthesis of Epoxidized Soybean Oil.....	14
2.2.2. Synthesis of Carbonated Soybean Oil.....	15
2.3. Characterization of ESBO and CSBO.....	17
2.3.1. Iodine Value.....	17
2.3.2. Epoxy Value.....	18
2.3.3. Fourier-Transform Infrared Spectroscopy.....	18
2.3.4. Nuclear Magnetic Resonance.....	19
2.3.5. Gel Permeation Chromatography.....	20
2.3.6. Viscosity.....	21
2.4. Characterization of NIPU films.....	22
2.4.1. Thermogravimetric Analysis.....	22
2.4.2. Differential Scanning Calorimetry Analysis.....	23
2.4.3. Dynamic Mechanical Analysis.....	24
2.4.4. Tensile Strength Measurement.....	25
2.4.5. Hardness.....	26
2.4.6. Water Contact Angle.....	27
<b>CHAPTER III.....</b>	<b>29</b>
<b>RESULTS AND DISCUSSION.....</b>	<b>29</b>
3.1. Characterization.....	29

3.1.1. Fourier-Transform Infrared Spectroscopy .....	29
3.1.2. Gel Permeation Chromatography .....	33
3.1.3. Nuclear Magnetic Resonance .....	33
3.2. Thermogravimetric Analysis .....	37
3.3. Differential Scanning Colorimetry .....	40
3.4. Dynamic Mechanical Analysis .....	44
3.5. Hardness and Tensile Strength.....	49
3.6. Degree of Swelling and Gel Content.....	53
3.7. Contact Angle Measurement .....	58
<b>CHAPTER IV .....</b>	<b>62</b>
<b>CONCLUSION.....</b>	<b>62</b>
<b>CHAPTER V .....</b>	<b>64</b>
<b>FUTURE WORK .....</b>	<b>64</b>
<b>REFERENCES .....</b>	<b>65</b>

## LIST OF TABLES

<b>Table 1:</b>	Decomposition temperatures for the NIPU containing EDA, BDA, and HDA.....	40
<b>Table 2:</b>	Transition temperatures for the NIPU containing EDA, BDA, and HDA for DSC and DMA.....	49
<b>Table 3:</b>	Young's modulus for the NIPU films obtained from different diamines with 24-hour curing time.....	53

## LIST OF FIGURES

<b>Figure 1:</b>	General reaction scheme for synthesis of PU.....	2
<b>Figure 2:</b>	General reaction mechanism for synthesis of PU.....	3
<b>Figure 3:</b>	General applications of PU.....	4
<b>Figure 4:</b>	Schematics for the synthesis of the NIPU films using different diamines.....	10
<b>Figure 5:</b>	Schematic of the preparation of NIPU films.....	16
<b>Figure 6:</b>	Digital photo of FT-IR instrument used in this research.....	19
<b>Figure 7:</b>	Digital photo of NMR instrument used in this research.....	20
<b>Figure 8:</b>	The GPC instrument used in this research.....	21
<b>Figure 9:</b>	Digital image of the viscosity instrument used in this research.....	22
<b>Figure 10:</b>	Digital photo of the TGA analysis instrument used in this research..	23
<b>Figure 11:</b>	Digital photo of the DSC instrument used in this research.....	24
<b>Figure 12:</b>	Digital photo of the DMA instrument used in this research.....	25
<b>Figure 13:</b>	Digital image of the tensile strength instrument used in this research.....	26
<b>Figure 14:</b>	Digital photo of the Hardness instrument used in this research .....	27
<b>Figure 15:</b>	Digital image of contact angle instrument used in this research.....	28
<b>Figure 16:</b>	FTIR spectra of (a)SBO, ESBO, and CSBO. (b) Different EDA to CSBO weight ratio at 6 hours. FTIR spectra were obtained from the increasing curing time for the NIPUs obtained from (c) EDA, (d) BDA, and (e) HDA (f) Decrease of epoxy concentration as a function of reaction time Decrease of epoxy concentration as a function of reaction time.....	32
<b>Figure 17:</b>	Chromatogram of ESBO and CSBO from GPC.....	33
<b>Figure 18:</b>	<sup>1</sup> H NMR spectra of SBO.....	35
<b>Figure 19:</b>	<sup>1</sup> H NMR spectra of ESBO.....	35
<b>Figure 20:</b>	<sup>1</sup> H NMR spectra for CSBO.....	36
<b>Figure 21:</b>	Proposed chemical structures after the reaction between CSBO and a diamine to form the NIPU film.....	36

<b>Figure 22:</b>	TGA and DTGA plots for the NIPU films cured at different times were obtained from the diamines (a, b) EDA, (c, d) BDA, and (e, f) HDA.....	39
<b>Figure 23:</b>	DSC for the NIPU films based on (a) EDA, (b) BDA, and (c) HDA.....	42
<b>Figure 24:</b>	DSC thermograms for the EDA, BDA, and HDA-based NIPU films at increasing curing times of (a) 1.5h, (b) 3h, (c) 6h, (d) 12h, (e) 24h.....	43
<b>Figure 25:</b>	DMA plots for EDA, BDA, and HDA-based NIPU films, respectively, for (a-c) tan delta.....	46
<b>Figure 26:</b>	DMA plots for EDA, BDA, and HDA-based NIPU films, respectively, for (a-c) storage modulus.....	47
<b>Figure 27:</b>	DMA plots for EDA, BDA, and HDA-based NIPU films, respectively, for (a-c) loss modulus.....	48
<b>Figure 28:</b>	(a) Hardness Shore D and (b) tensile strength tests for the NIPU films. (c) Stretchability of the NIPU films during tensile testing. (d) Various aspects of the NIPU film's flexibility. (e) Bone-shaped specimen used for the tensile test.....	52
<b>Figure 29:</b>	Proposed cross-linking structure of urethane bond.....	53
<b>Figure 30:</b>	Degree of swelling for the NIPU films at increasing curing times at (a) DMSO, (b) NMP, (c) DMF, and (d) toluene.....	55
<b>Figure 31:</b>	Gel content for the NIPU films at increasing curing times at (a) DMSO, (b) NMP, (c) DMF, and (d) toluene.....	57
<b>Figure 32:</b>	The physical aspect of the swollen NIPU films after drying.....	58
<b>Figure 33:</b>	Contact angles for the 24h cured EDA, BDA, and HDA-based NIPU films in for (a) water, (b) glycerol, (c) ethylene glycol, (d) dimethyl sulfoxide, and (e) dimethyl formamide.....	60

## LIST OF ABBREVIATION

BDA	1,4-Butylene Diamine
CO <sub>2</sub>	Carbon Dioxide
CSBO	Carbonated Soybean Oil
DMA	Dynamic Mechanical Analysis
DMF	Dimethyl Formamide
DMSO	Dimethyl Sulfoxide
DS	Degree of Swelling
DSC	Differential Scanning Calorimetry analysis
EDA	1,2-Ethylenediamine
ESBO	Epoxide Soybean Oil
FT-IR	Fourier-Transform Infrared Spectroscopy
GC	Gel Content
GPC	Gel Permeation Chromatography
NIPU	Non-Isocyanate Polyurethanes
NMP	N-methyl-2-Pyrrolidone
NMR	Nuclear Magnetic Resonance
PU	Polyurethane
SBO	Soybean Oil
TBAB	Tetrabutylammonium Bromide
TGA	Thermogravimetric Analysis

## **CHAPTER I**

### **INTRODUCTION**

#### **1.1. Background of Polyurethanes**

Polyurethanes (PUs), derived from the creative work of chemists in the 1930s, have evolved into versatile polymers with a long history. Initially discovered through the synthesis of isocyanates, these materials took center stage during World War II, proving to be invaluable for military applications. PU has found application in a variety of widely used products, including foams, coatings, adhesives, and elastomers. The development of PU coatings in the 1950s was a breakthrough moment, paving the path for broad application in construction, automobiles, and other consumer goods. A common process for producing PU materials involves the reaction of polyol and isocyanate, followed by a polyaddition reaction that results in the development of a urethane linkage bond. This conventional process relies on petroleum-based polyol and isocyanate. In the late 1980s and 1990s, the utilization of various isocyanates lead to rapid and substantial growth in the PU industry. In the early years of the 21<sup>st</sup> century, polyurethane industries had the fastest growth among all chemical sectors [1].

## 1.2. Chemistry of Polyurethanes

PU has repeating units of monomers in a polymeric material. The conventional method to produce PU is the reaction between a diol (HO-R-OH) and di-isocyanate (OCN-R-NCO), which produces the urethane (-NHCOO-) linkage as shown in **Figure 1** [2,3]. To make PU both the starting materials must have more than two functionalities. PUs are block copolymers that alternate between soft and hard segments. Soft segments are frequently manufactured from polyether or polyester polyols, whereas hard segments are formed by converting diisocyanate to urethane. Moreover, isocyanates are classified into two subgroups: aliphatic and aromatic. Aromatic isocyanates are more reactive and stiffer, resulting in highly cross-linked polyurethane matrices. Aliphatic isocyanates react slower with polyols, resulting in flexible and UV-stable PU matrices. Generally, the reaction between polyol and diisocyanate is exothermic. PU's adaptability derives from its combination of hard and soft parts, making it appropriate for various applications [4].

**Figure 2** shows a general reaction and mechanism for the synthesis of PU [5].

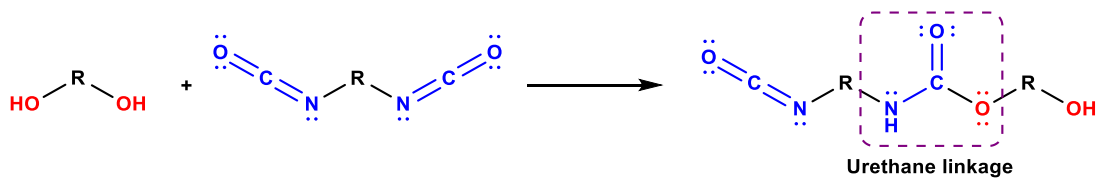


**Figure 1.** General reaction scheme for the synthesis of PU.

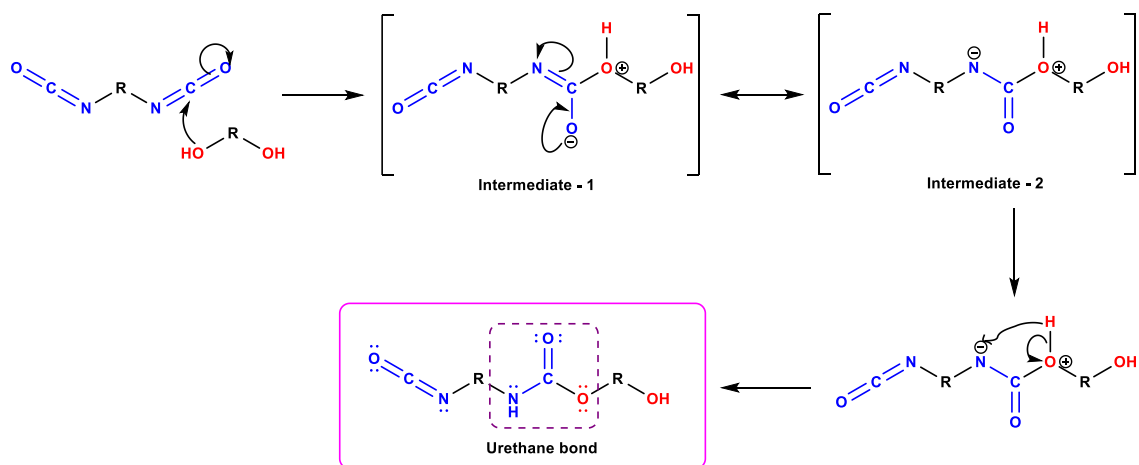


**Figure 1.** General reaction mechanism for synthesis of PU.

### 1.3. Properties and Applications of Polyurethane Materials

Generally, the properties of PU vary based on the types of polyols and isocyanates used. The polymer's properties can be substantially modified by adjusting parameters such as chain length, molecular weight, functional groups, and functionalization of the polyol chain with elements like halogens and acrylics. Based on the material parameters and the unique properties of the urethane bond, PU materials can show various characteristics and properties such as water and chemical resistance, thermal stability, and durability. This wide range of customization makes PU a versatile material, valuable in many industrial applications. As shown in **Figure 3**, a wide range of PU materials have potential applications in different sectors such as films, coating, adhesives, foam, automotive, medical textile, and construction [6–15].

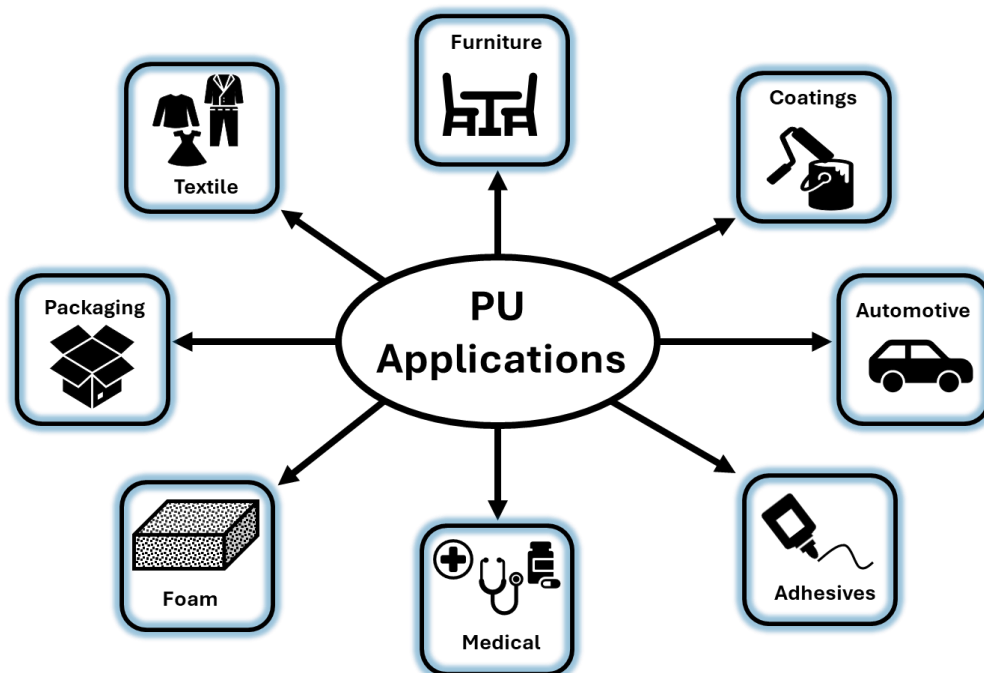


**Figure 2.** General applications of PU.

### 1.3.1 PU Films

Polymeric films have wide applications in every sector such as coating, packaging, electronics, automobiles, and medicine [16]. All PUs fall into one of two categories: thermosets or thermoplastics. After curing, thermoset PUs cannot be remelted or reshaped by heating because their curing process involves irreversible chemical changes. Thermoset PUs typically have high heat resistance, dimensional stability, and excellent chemical resistance. Thermoset films are used in electronic circuit boards, aerospace components, and automotive parts. The strength and surface morphology of epoxy coatings, along with the effects of inorganic oxide nanoparticles and halloysite, were analyzed by Shi et al. to develop a homogeneous epoxy coating aimed at enhancing the anti-corrosion properties of steel [17]. For better coating properties, self-healing is deemed the optimal approach for

reducing maintenance costs. Kim et al. synthesized self-healing and corrosion protection film for marine environments from bromo butyl rubber and carbon nanotubes [18]. Conversely, thermoplastic materials can be softened and reshaped when heated, and resolidify upon cooling, with the result that thermoplastic PU films can be reused with less environmental cost. Thermoplastic PUs offer a range of properties, including flexibility, transparency, and chemical resistance depending on the starting material used. Thermoplastic films are generally used in packaging [19], which include polyethylene (PE) films, polypropylene (PP) films, polyvinyl chloride (PVC) films, polyester (PET) films, and polyurethane films [20,21]. By incorporating nanofiller, some PU films can show conductance, and this is how these films can be used in electrical circuit boards [22].

### **1.3.2. PU Adhesive and Coating**

An adhesive is a substance that is applied to one or both surfaces of two distinct objects, binding them together and preventing them from being separated. PU adhesives are recognized for their excellent bonding properties, versatility, and resistance to various environmental conditions such as moisture, heat, and chemicals [23]. Its applications include wood flooring, construction and building materials, the automotive sector, electronics and electrical applications, packaging and labeling, medical and healthcare, furniture, security tapes, and binding paper. The coating is a thin layer of liquid that can be applied to surfaces for two primary purposes: protection and decoration. PU coatings are generally used in a variety of applications such as decorative finishes, the automobile industry, architectural coatings (exterior and interior paints), industrial coatings (marine, oil and gas, and chemical processing industries), and wood coatings due to their unique

properties like corrosion protection, chemical and weather resistance, and anti-fouling properties [24].

### **1.3.3. PU Foam**

Foams account for over half of all PU applications and are classified into two types: flexible foam and rigid foam, due to variations in structure, density, and flexibility [25]. Flexible foams are often used in applications such as beds, couches, vehicle seats, automotive interior design, footwear, and carpet underlay where comfort and cushioning are essential due to their flexibility. However, rigid polyurethane foams are employed in insulation applications such as insulation panels, freezers and refrigerators, building insulation, furniture, and energy-efficient transportation due to their excellent insulating qualities and closed-cell content [26].

### **1.3.4. Elastomer**

Elastomers are rubber-like polymer compounds that have high elasticity and durability. They are used in a range of applications, including automotive (tires), medical equipment (e.g., cardiac-assist pumps and blood bags), and chronic implants (e.g., heart valves and vascular grafts), because of their ability to deform and return to their original shape after stress [27].

Considering the importance of PU application in every sector and the consumption of isocyanates and petroleum-based products, its preliminary requirements are to focus on the drawbacks of conventional PU for the environment and human life.

#### **1.4. Drawbacks of Conventional Polyurethanes**

The conventional method for synthesizing PU is the reaction between polyol and isocyanate, where both the starting compounds are sourced from petroleum. This feedstock is a non-renewable resource and is a significant contributor to the carbon footprint [28]. At the same time, isocyanate is harmful to the environment and human health due to its preparation route, which involves many toxic chemicals such as phosgene, methyl amine hydrochloride, and carbamyl chloride [29]. Along with the preparation process, isocyanate exhibits high reactivity, reacting with different chemicals and releasing toxic byproducts. Moreover, when -NCO reacts with moisture or water, it releases CO<sub>2</sub> gas, which is a significant contributor to global warming [30]. According to a toxicity study of different isocyanates butane diisocyanate releases putrescine, which belongs to the amine class generally formed from protein degradation, and in large quantities is dangerous for human life. Commonly used isocyanates, such as toluene diisocyanate or MDI, are highly hazardous during both manufacturing and degradation, releasing carcinogenic diamines. Inhaling isocyanate vapors is the most hazardous form of human exposure, leading to respiratory illnesses [31].

#### **1.5. Bio-based Polyurethane**

To address the issue of petroleum product scarcity and carbon footprints alternative, eco-friendly routes for PU production are being actively explored with an emphasis on the development of a green synthesis approach that uses sustainable and renewable sources such as vegetable oil [32], cellulose, polysaccharides [33], and carbohydrates [34]. Most research currently uses vegetable oils containing fatty acids (aliphatic long chain), which can be functionalized by many chemical methods such as hydroformylation, ozonolysis,

amidation-esterification, and epoxidation-ring opening [35]. This approach is being explored on a large scale by many companies such as Dow Chemical, Bayer Material Science, and Shell. Furthermore, many routes have been explored to prepare bio-based isocyanate from fatty acids, lignin amino acids and amino bases, algae, and saccharides. From fatty acid Hojabti et al. [36] reported the preparation of diisocyanate from 9-Oxononanoic Acid, In this process oleic acid was converted to diacid and was reacted with ethyl chloroformate and sodium azide to get 1,7-heptamethylene diisocyanate 4 (HPMDI). In 1980s Glasser et al. [37] first reported the preparation of diisocyanate from lignin, in this method acid group was converted into acid chloride in the next step reaction with sodium azide. Dry and wet heating were used to obtain isocyanate followed by Curtius rearrangement. A variety of bio-based isocyanates are commercially available from many companies such as Vencoex, Covestro, and Mitsui Chemical [31]. However, finding bio-based routes to produce isocyanate is not sufficient to preserve the environment. It is necessary to make urethane linkage and develop an environmentally acceptable PU from an isocyanate-free approach. The aim of this research is to create an eco-friendly and sustainable PU film by avoiding the usage of petroleum-based polyols and isocyanates.

### **1.6. Non-isocyanate Polyurethane**

Generally, non-isocyanate polyurethane (NIPU) is synthesized by reacting a cyclic carbonated group with a primary amine to form the urethane linkage [38–40]. A cyclic carbonated group can be generated by reacting epoxy and CO<sub>2</sub>. To do this, the epoxy groups can be chemically introduced into an unsaturated vegetable oil by epoxidation, and then CO<sub>2</sub> can be used as a reagent to convert the epoxy into a cyclic carbonate. The use of readily available renewable materials such as CO<sub>2</sub> and soybean oil (SBO) makes this

process highly sustainable. In a further step, the primary amine reacts with the cyclic carbonated monomer to yield the urethane linkage [41]. Because this process does not require isocyanates, this is a more sustainable way to synthesize PUs. PUs can open several possibilities for the fabrication of a wide set of NIPUs with different properties, which can be obtained by varying the catalysts [42–45] utilizing multifunctional carbonates, compositing with inorganic materials, or other polymers [45–48]. Such variety allows for the design of polymeric structures that can potentially cover a broad range of applications.

### **1.7. Research Objective**

This work presents the synthesis and characterization of a NIPU derived from SBO by converting the double bonds in the SBO into epoxy groups, ESBO, followed by a reaction with CO<sub>2</sub> to obtain the carbonated soybean oil (CSBO). Then, three diamines ethylene diamine (EDA), butylene diamine (BDA), and hexene diamine (HDA), were reacted with the CSBO to obtain NIPU films. The reaction scheme for the synthetic process and the proposed chemical structures are presented in **Figure 4**. When the structure-property relation and thermo-mechanical properties of the NIPUs were analyzed, the material was shown to have beneficial thermal, mechanical, and hydrophobic properties which suggests that it has the potential for industrial application. The novelty of this work is in the use of eco-friendly and renewable materials to synthesize a flexible NIPU with mechanical properties. The synthesis of the CSBO utilizes CO<sub>2</sub>, which can function to capture carbon from the environment while using an abundant renewable starting material to synthesize the monomers for the NIPU. Lastly, the synthesis of the NIPU uses a solvent and catalyst-free method consisting of the direct addition of different aliphatic diamines followed by mixing and curing to obtain the polymeric films [49,50].

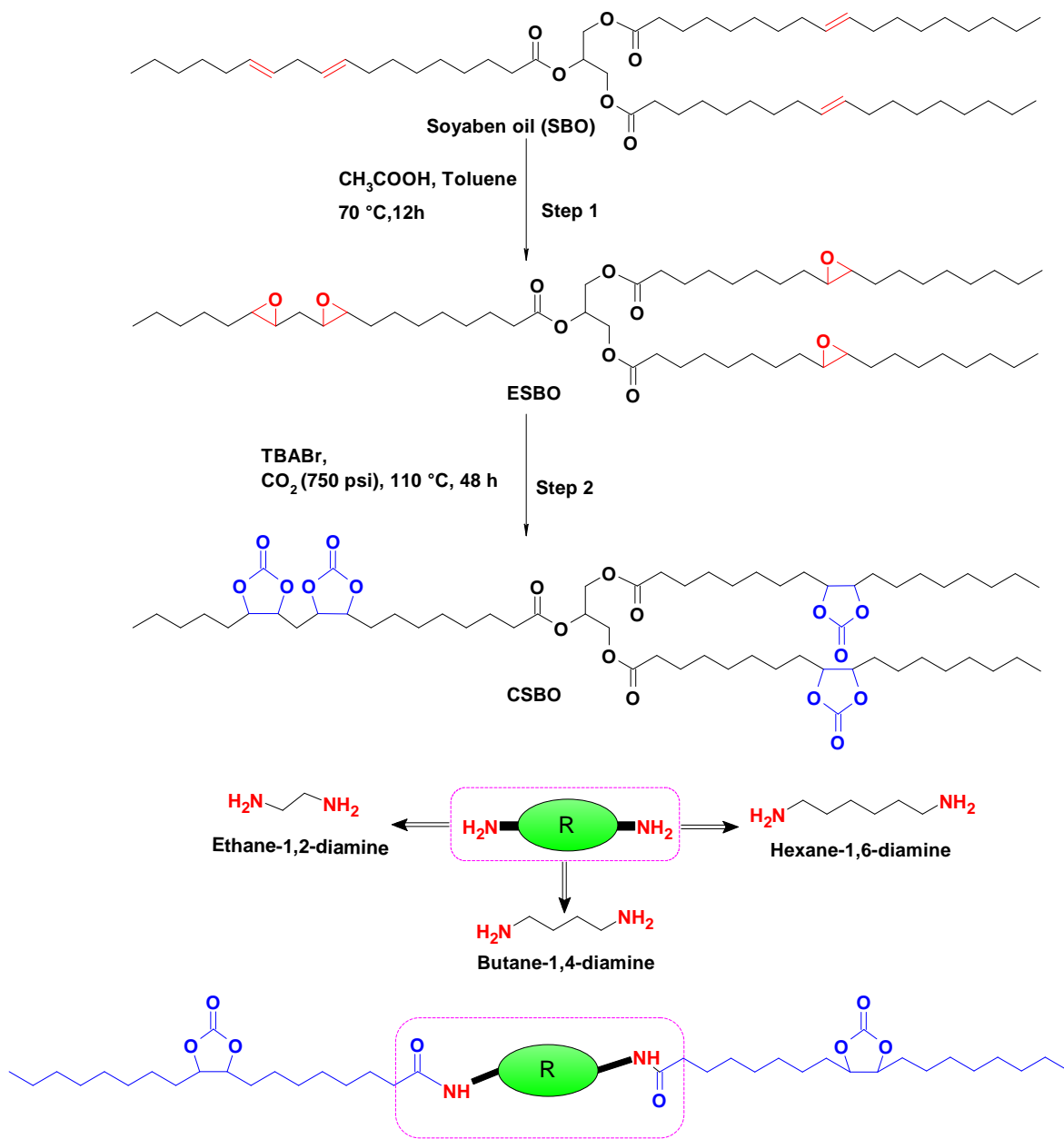


**Figure 3.** Schematics for the synthesis of the NIPU films using different diamines.

## CHAPTER II

### MATERIALS AND METHODS

#### 2.1. Materials

Soybean oil and distilled water were purchased from a local Walmart (Pittsburg, KS, USA). Glacial acetic acid (99.7%), toluene (99.5%), Amberlite IR 120H, sodium chloride, sodium sulfate, and tetrabutylammonium bromide (TBAB) (99%) were purchased from Sigma-Aldrich (Basking Ridge NJ, USA). Hydrogen peroxide 30% (w/w), EDA, BDA, and HDA were purchased from Sigma-Aldrich (St. Louis, MO, USA). CO<sub>2</sub> was supplied by Matheson Trigas (Basking Ridge, NJ, USA).

##### 2.1.1. Soybean Oil

SBO is derived from the seeds of the glycine max plant, often referred to as soybean. SBO consists of saturated, monounsaturated, and polyunsaturated fats. SBO is rich in unsaturated fatty acids, namely triglycerides. This material comprises 51% polyunsaturated linoleic acid and 7-10% alpha-linoleic acid. Furthermore, it contains a significant amount of monounsaturated oleic acid, accounting for 23% of its overall makeup. The primary objective of the study was to convert the C=C bonds present in SBO triglycerides into an epoxy ring that could be used for further synthesis [51]. The SBO employed in this experiment was obtained from a neighboring Walmart in Pittsburg, KS,

USA, and used without any further processing. The viscosity of SBO at ambient temperature was measured to be 0.19 Pa.s. **Figure 4** displays the chemical composition of SBO. The primary objective of this study was to enhance the reactivity of the carbon-carbon double bond present in the triglycerides of SBO. This was done to create more reactive sites that may be used for further synthesis. The research used SBO as the primary material for synthesizing bio-based polyurethane films.

### **2.1.2. Tetrabutylammonium Bromide**

TBAB, a quaternary ammonium salt with the chemical formula  $(C_4H_9)_4NBr$ , serves as a versatile phase transfer catalyst in organic chemistry reactions. It is excellent for promoting reactions, which follow nucleophilic substitution in nonpolar solvents. TABA catalyst can also be used for alkylation, oxidation, reduction, and esterification processes. In addition, TBAB is a good co-catalyst in a variety of coupling processes. Furthermore, it performs well as a zwitterionic solvent in a variety of organic transformations carried out under molten conditions.

### **2.1.3. 1,2, Ethylene Diamine**

EDA, with the chemical formula  $NH_2CH_2CH_2NH_2$ , is a colorless, strongly alkaline liquid widely used as a versatile building block in chemical synthesis. Due to its stable bond formation with metal ions, it is widely used in agriculture, textile processing, and water treatment, and it is known as a chelating agent. Moreover, it works as an important intermediate in organic synthesis compounds, including polymers, and pharmaceuticals. Due to the highly reactive nature of its primary ( $-NH_2$ ) groups on both sides, this compound

can serve as a crosslinking agent in resin and polymer production, thereby enhancing mechanical properties and stability.

#### **2.1.4. 1,4-Butane Diamine**

BDA, commonly known as putrescine, is a diamine characterized by the chemical formula  $\text{NH}_2(\text{CH}_2)_4\text{NH}_2$ . This white semi-solid substance emits a slight amine odor and is found naturally in organisms. It is an important monomer in polymer production, particularly in the chemical industry, where it is used to synthesize polyamides and epoxy resins. Furthermore, putrescine holds potential applications as a corrosion inhibitor and is subject to exploration for its possible uses in pharmaceuticals and agricultural products.

#### **2.1.5. 1,6, Hexamethylene Diamine**

HDA is a key chemical compound with diverse industrial applications. Comprising a six-carbon chain with amino groups at each end, it holds pivotal roles in several processes. One primary use is in the manufacturing of nylon 6,6, a widely employed synthetic polymer in textiles, automotive parts, and engineering plastics. By reacting with adipic acid, HDA forms the polymer chain essential for nylon production. Moreover, HDA serves as a foundational element in creating other polymers and resins, such as polyamides, polyurethanes, and polyesters, through condensation reactions with various monomers. Additionally, its utilization as a curing agent in epoxy resins enhances material strength and durability by facilitating cross-linking. With its corrosion inhibition properties, HDA contributes to coatings and metal treatments, while also finding application in pharmaceuticals for synthesizing medications like antibiotics and antifungal agents. Thus,

owing to its versatility and chemical characteristics, HDA plays an indispensable role across diverse industrial sectors.

### **2.1.6. Carbon Dioxide**

CO<sub>2</sub> is a naturally occurring, colorless, and odorless gas comprised of one carbon atom bonded to two oxygen atoms. It plays a vital role in Earth's carbon cycle, being produced through natural processes like respiration and volcanic activity, as well as human activities such as burning fossil fuels and deforestation. While essential for photosynthesis in plants, excessive carbon dioxide emissions contribute to global warming and climate change by enhancing the greenhouse effect. Consequently, efforts to reduce carbon dioxide emissions and enhance carbon sequestration are crucial for mitigating climate change impacts. Beyond its environmental significance, carbon dioxide is utilized in various industrial applications, including carbonating beverages, as a fire extinguisher, and in chemical synthesis.

## **2.2. Synthesis**

### **2.2.1. Synthesis of Epoxidized Soybean Oil**

A commercially available SBO (100 g) was charged in a four-necked round bottom flask equipped with a mechanical stirrer. Then, the SBO was diluted with 50 mL of toluene. After that, 25 g of Amberlite IR 120H resin was added to the solution and cooled down at 0 °C with vigorous stirring. After cooling, glacial acetic acid (14.9 g, 0.248 mol, 0.5 eq.) was added dropwise and the reaction mixture was stirred for 30 min at 0 °C. Then 30% hydrogen peroxide (84.33 g, 0.744 mol, 1.5 eq.) was added to the reaction mixture. After complete addition, the system was heated to 70 °C for 7 h. After the completion, the

reaction mixture was allowed to cool down to room temperature. After that, the resin was filtered out with the help of a 50  $\mu\text{m}$  filter with nylon mesh. The remaining oil was washed with brine several times. Later, the organic layer was dried over sodium sulfate and concentrated under reduced pressure to collect ESBO. The obtained product was confirmed through FT-IR and GPC. After that, the ESBO was used in the synthesis of CSBO.

### 2.2.2. Synthesis of Carbonated Soybean Oil

**Figure 5.** shows 1000 mL autoclave reactor. In an autoclave reactor, ESBO (100 g) and TBAB (3.7 g, 0.011 mol, 0.27 eq.) catalysts were mixed and stirred at 1100 rpm. Then,  $\text{CO}_2$  gas was purged through low pressure in the reaction mixture three times. After a uniform environment was established, the system was gradually heated up to 110  $^\circ\text{C}$  and initially set at a pressure of 300 psi. After that,  $\text{CO}_2$  pressure rose to 800 psi for 36 h. The reaction progress was monitored through oxirane oxygen percentage (EOC %) and viscosity analysis. For the EOC % wet chemistry analysis, the sample was dissolved in glacial acetic acid in the presence of tetraethylammonium bromide. Then, crystal violet was used as an indicator and the solution was titrated with 0.1 N  $\text{HClO}_4$  until it transitioned from blue to the green endpoint. The EOC % was calculated based on Equation 1.

$$\text{EOC (\%)} = \frac{V \times N \times 1.6}{\text{Wt. sample}} \quad (1)$$

Where,  $V$  and  $N$  are the volume for titration and the normality of  $\text{HClO}_4$ , respectively. During the reaction, small aliquots were taken from the reaction system to monitor its progress. That step was done by gently opening a valve connected to a tube inserted into

the reaction mixture. Through that, small aliquots could be collected without interfering with the system or causing variations in the internal pressure.

### 2.2.3. Synthesis of Non-Isocyanate Polyurethane Film

To fabricate the NIPU films, diamine (20.5 wt.% of CSBO) and CSBO were added at room temperature and gently mixed with a glass rod, to avoid air bubbles, until the mixture became viscous. Simultaneously, a Teflon mold was prepared by spraying mold releaser followed by heating it at 85 °C. After that, the viscous mixture was poured into a mold and cured at 85 °C at different curing times of 1.5, 3, 6, 12, and 24 h as shown in **Figure 6**.

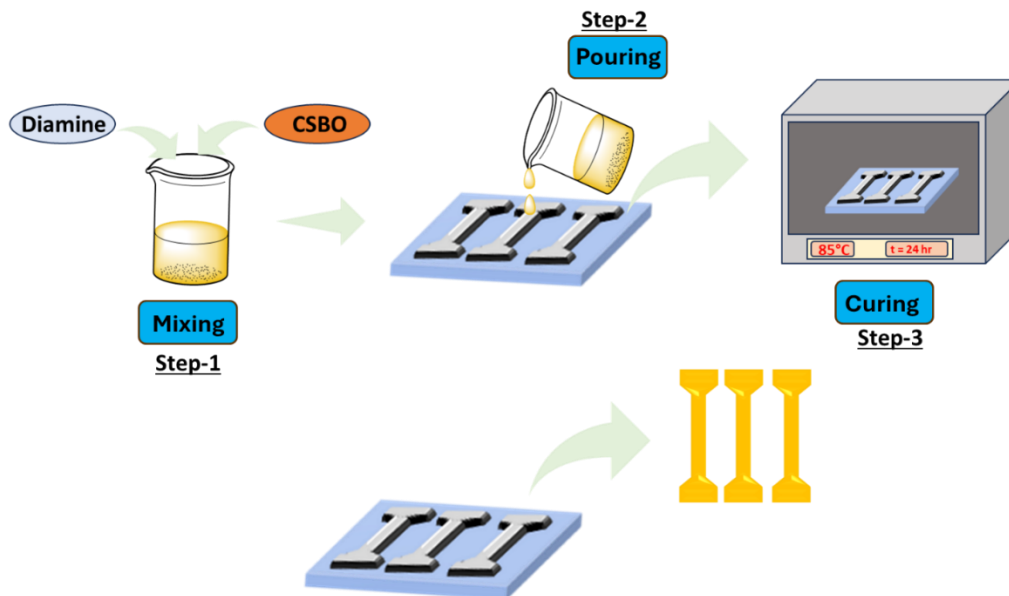


**Figure 5.** Schematic of the preparation of NIPU films.

## 2.3. Characterization of ESBO and CSBO

### 2.3.1. Iodine value

The iodine value (IV) represents the degree of unsaturation available in any fatty acid or oil. IV is the amount of iodine that can react to form double bonds per 100 grams of oil. This study employed IV to count the number of double bonds in the initial SBO, and intermediate ESBO. IV can be calculated via the titration method by following the Hanus method (IUPAC 2.205) standard procedure. To determine the IV, 0.2 gm of SBO was taken into a 250 ml conical flask, which was covered with aluminum foil to protect it from light, and the sample was diluted with 10 ml  $\text{CHCl}_3$ . After the homogeneous solution, 20 ml of Hanus reagent was then added, shaken gently, and kept in a dark place for an hour. After completion of one hour, 20.0 ml of 10% potassium iodide solution, 50.0 ml of HPLC grade water, and six drops of the starch indicator were added. The mixture was titrated with aqueous sodium thiosulfate ( $\text{NaS}_2\text{O}_3$ ) solution with vigorous shaking until the solution became colorless.

$$Iv = 12.69 \times T \times (Va - Vb) / W \quad (2)$$

Finally, IV was calculated using equation 2, where T is the normality of the Hanus reagent, Va is the  $\text{NaS}_2\text{O}_3$  volume for the sample, Vb is the  $\text{NaS}_2\text{O}_3$  volume for the blank, and W is the sample weight. The IV of SBO was 126.40 gm  $\text{I}_2$ /100 gm oil, which means that 0.4 molecules of double bonds were present in 100 gm of SBO sample.

### 2.3.2. Epoxy Value

The epoxy oxygen content (EOC %) was assessed using a combination of glacial acetic acid and TBAB. This method allowed the scrutiny and confirmation of epoxide group formation from double bonds. For the analysis, 0.3 g of ESBO was diluted in a 50 mL solution of TEAB. The solution was titrated with 0.1 N perchloric acid (HClO<sub>4</sub>), incorporating a crystal violet indicator. Titration concluded upon the observation of a color change from blue to green. The resulting volume was utilized to determine the epoxy content in the ESBO, based on the average of three tests.

### 2.3.3. Fourier-Transform Infrared Spectroscopy

Fourier-transform infrared spectroscopy is a quick and efficient method for detecting functional groups in a chemical molecule. This technique is used for obtaining the infrared spectrum of a solid, liquid, or gas's absorption or emission. Unlike other tests, it eliminates the need for sample purification and doesn't utilize solvents. FTIR spectroscopy has been utilized in various areas, including chemistry, materials science, pharmaceuticals, food analysis, and environmental monitoring. The materials' FTIR spectra were recorded using a PerkinElmer Spectrum Two Spectrophotometer (**Figure 6**). The scans spanned the spectrum range of 4000-400 cm<sup>-1</sup> with a resolution of 4 cm<sup>-1</sup> and an average of 64 scans, allowing for a quick and thorough study of the chemical composition.



**Figure 6.** Digital photo of FT-IR instrument used in this research.

#### **2.3.4. Nuclear Magnetic Resonance**

Nuclear Magnetic Resonance (NMR) spectroscopy is widely used in chemical analysis to identify and characterize inorganic as well as organic compounds. It depicts the molecular structure, chemical environment, and atom connections inside a molecule. At its foundation, NMR is based on the behavior of atomic nuclei when exposed to a high magnetic field and radiofrequency radiation. When exposed to a magnetic field, some nuclei, such as hydrogen or carbon, align themselves in two energy states. The nuclei can be stimulated by applying radiofrequency radiation at the resonance frequency corresponding to the energy difference between these states, and the NMR spectrometer detects their responses. The Magritek spinsolve 80 MHz NMR Spectrophotometer as shown in **Figure 7** was utilized to obtain spectral data for synthesized materials.

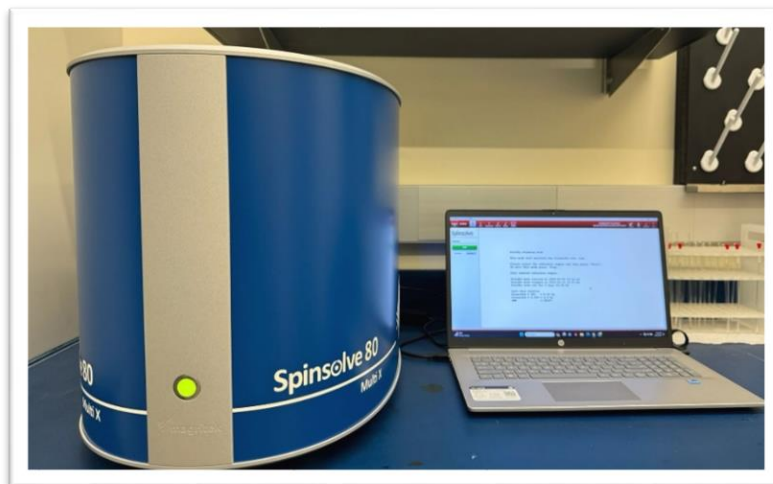


**Figure 7.** Digital photo of NMR instrument used in this research.

### **2.3.5. Gel Permeation Chromatography**

Gel permeation chromatography (GPC), also known as size exclusion chromatography, stands as a pivotal technique in polymer science, enabling the separation and analysis of macromolecules based on their size in solution. Particularly instrumental in polymer characterization, GPC's ability to differentiate polymers according to molecular size provides crucial insights into the distribution of molecular weights within a polymer sample. This information is essential for assessing polymer quality, understanding synthesis processes, and predicting material properties. In the polymer sector, GPC plays a key role in quality control, ensuring the consistency of polymer batches and aiding in the characterization of complex hydrocarbons. In this study, the GPC instrument from Waters, located in Milford, MA, USA, was employed, as illustrated in **Figure 8**. Additionally, tetrahydrofuran (THF) served as the solvent, flowing at a rate of 1 mL/min and maintained at a temperature of 30 °C.



**Figure 8.** The GPC instrument used in this research.

### 2.3.6. Viscosity

Viscosity, an important indicator of a substance's resistance to flow, can provide essential details about its molecular weight; low viscosity indicates a lower molecular weight, whereas high viscosity may indicate a higher molecular weight. Furthermore, reduced viscosity is frequently related to higher processability. In this experiment, the viscosity of CSBO increased as compared to ESBO and SBO. Furthermore, the viscosity parameter plays an important role in determining the correct production of the CSBO utilizing soybean epoxide. **Figure 9** shows the study using an AR 2000 dynamic stress rheometer from TA Instruments, USA. Viscosity measurements were taken at 25 °C, with shear stress gradually increased from 1 to 2000 Pa linearly. The dynamic rheometer was supplied with a cone plate with a 2° angle and a 25 mm diameter. It is especially

important in different polymer processing processes such as extrusion, injection molding, and fiber spinning.



**Figure 9.** Digital image of the viscosity instrument used in this research.

## **2.4. Characterization of NIPU films**

### **2.4.1. Thermogravimetric Analysis**

Thermogravimetric analysis is a technique for determining the thermal stability of materials by heating them at an even rate and measuring the weight change of the sample with temperature. To assess the thermal stability of NIPU films with varying diamine and different curing times, samples were subjected to analysis using the TGA instrument (Q500, Discovery, Trios, USA), as illustrated in **Figure 10**. A sample of approximately 5-10 mg was placed on an aluminum pan and the test was conducted under nitrogen flow at a ramp rate of 10°C/min within a temperature range of 25–600°C.

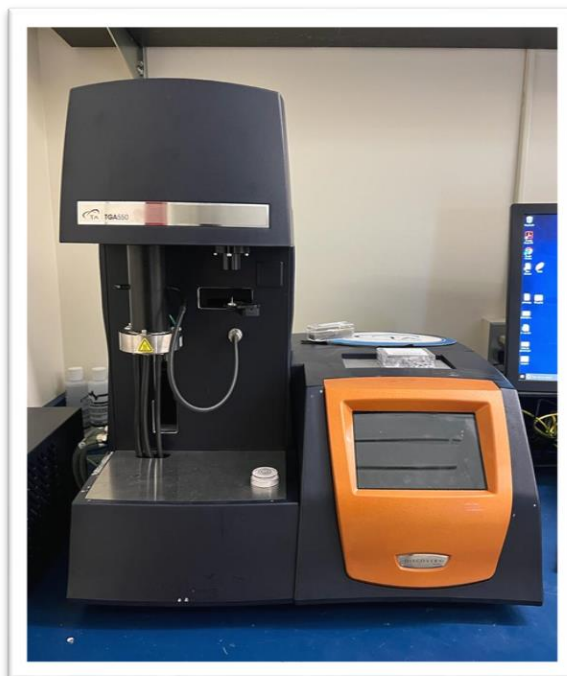


**Figure 10.** Digital photo of the TGA analysis instrument used in this research.

#### **2.4.2. Differential Scanning Calorimetry Analysis**

Differential scanning calorimetry is an instrument used for thermal analysis to evaluate changes in the physical characteristics of samples and their temperature over time. This instrument is primarily used to measure glass transition temperatures ( $T_g$ ), melting temperatures ( $T_m$ ), and crystallization temperatures ( $T_c$ ). All the DSC tests for this study were carried out using the DSC Q100 instrument (TA Instruments, USA) as shown in **Figure 11**. All the tests were performed in the temperature range of -80 to 300 °C with a ramp rate of 10 °C per minute. DSC gives understanding by measuring thermal stability, identifying phases, and separating between amorphous and crystalline regions. It is useful to understand how chemicals are distributed in different crystal structures.



**Figure 11.** Digital photo of the DSC instrument used in this research.

### **2.4.3. Dynamic Mechanical Analysis**

Dynamic Mechanical Analysis (DMA) is a method used to assess the mechanical properties of materials in relation to various factors such as temperature, time, and frequency. This enables researchers to analyze parameters like storage modulus, loss modulus, and damping properties, providing valuable insights into the viscoelastic behavior and mechanical performance of the material under different conditions. DMA finds widespread applications across fields including materials science, polymer research, and engineering for studying the behavior of polymers, composites, and other materials. In this study, TA instrument (TGA Q-800), was used as shown in **Figure 12**.



**Figure 12.** Digital photo of the DMA instrument used in this research.

#### **2.4.4. Tensile Strength Measurement**

Tensile strength equipment evaluates the tensile characteristics of materials such as metals, plastics, rubbers, fabrics, composites, and ceramics. This comprises calculating tensile strength, yield strength, modulus of elasticity, elongation at break, and ultimate tensile strength. This is necessary for understanding how materials react under strain and creating materials for certain uses. The tensile strength test was performed by using an Instron 3367 following the ASTM D882-97 Standard. The specimens were films of around with dimensions of 50 mm of length, 10 mm of uniform width, and thickness of around 2.45 mm. The test was performed at a rate of 10 mm/min. **Figure 13** shows the lap shear strength instrument used in this research.

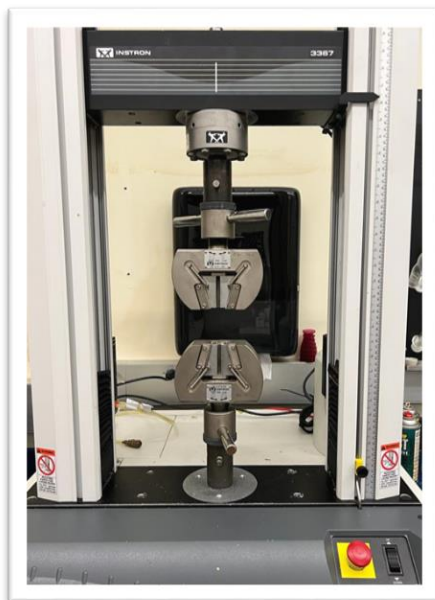


**Figure 13.** Digital image of tensile strength instrument used in this research.

#### **2.4.5. Hardness**

Hardness, a pivotal aspect in the assessment of film properties, particularly its impact resistance, is determined through testing. The application of the requisite load for film penetration is carried out using the Type D Durometer from PTC instruments, following the guidelines of ASTM D2240 (**Figure 14**). The film is punctured with the instrument's sharp point through the application of force, and the resulting hardness is then observed on the dial of the instrument.



**Figure 14.** Digital photo of the Hardness instrument used in this research.

#### **2.4.6. Water Contact Angle**

In material characterization, the water contact angle is frequently employed, particularly for polymers, coatings, and thin films. This information is deemed crucial for understanding how a material will interact with liquids in practical applications. The investigation of surface energy and wettability using water contact angle instruments involves measuring the contact angle of a specific chemical droplet on a surface, allowing the determination of the material's hydrophobic or hydrophilic nature. This combined approach provides a comprehensive understanding of the material's surface properties, aiding in the design and optimization of materials for various applications. The water contact angle was measured by using an Ossila Contact Angle Goniometer (**Figure 15**). Every analysis was performed at least twice, and an average value was reported.

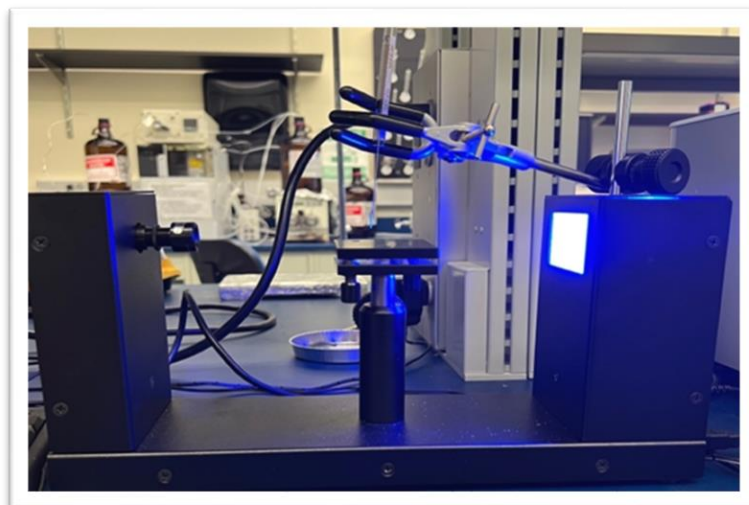


**Figure 15.** Digital image of contact angle instrument used in this research.

## CHAPTER III

### RESULTS AND DISCUSSION

#### 3.1. Characterization

##### 3.1.1. Fourier-Transform Infrared Spectroscopy

**Figure 16(a)** shows the FT-IR spectra for the SBO, ESBO, and CSBO. For the case of SBO, it could be observed a small peak at  $3009\text{ cm}^{-1}$  assigned to the H-C=C stretch. In the ESBO spectra, the H-C=C peak at  $3009\text{ cm}^{-1}$  disappeared whereas a new peak related to the C-O-C bending around  $844\text{ cm}^{-1}$  appeared which suggested the conversion of the unsaturation from the vegetable oil into epoxy rings [52]. In the CSBO spectra, there was the appearance of a peak around  $1800\text{ cm}^{-1}$  assigned to the C=O stretch from the cyclic carbonated group along with the disappearance of the peak at  $844\text{ cm}^{-1}$ . Also, the peak at around  $1700\text{ cm}^{-1}$  has been attributed to the C=O stretch of the ester group [40]. **Figure 16(f)** displayed the decrease in epoxy concentration over time for the carbonation reaction, which showed that after around 40 h, the epoxy groups were completely consumed from the system. After the reaction was completed, it was allowed to cool down to  $50\text{ }^{\circ}\text{C}$ . After that, the pressure was slowly released from the system. Finally, a light brown viscous waxy liquid was obtained.

**Figure 16(b)** presented the FTIR for NIPUs containing increasing concentrations of EDA that were measured after 6h of reaction. It could be observed that when concentrations above 20.5 wt.% of EDA concerning CSBO were utilized to react with the CSBO there was a disappearance of the sharp peak around  $1800\text{ cm}^{-1}$  assigned to the C=O stretch related to the carbonated groups. Simultaneously, there was also the appearance of the N-H stretch at  $3300\text{ cm}^{-1}$  which suggested the presence of amine groups. Also, there were two peaks at  $1632$  and  $1540\text{ cm}^{-1}$  which were assigned to CONH and C-N stretch, respectively, that suggested the presence of amides. Lastly, the peak from around  $1710$  to  $1733\text{ cm}^{-1}$  could be attributed to the presence of urethane groups [40,53]. Based on that, it could be observed that the increasing wt.% of EDA led to a continuous decrease in the sharp peak around  $1800\text{ cm}^{-1}$  assigned to C=O stretch from cyclic carbonated groups, suggesting their reaction with the diamine. From that, the addition of 20.5 wt.% of EDA in relation to CSBO led to the consumption of the cyclic carbonates, given their disappearance in the FTIR spectra after a curing process of 6h. It is worth noting that, the curing process occurred at  $85\text{ }^{\circ}\text{C}$  which could function as enough driving force for the reactions to occur. Yet, it could be likely that several reactions could take place considering that the diamines could react with cyclic carbonates, carbonyls from the triglycerides, and leftover epoxies [53,54]. Given that situation, 20.5 wt.% of CSBO was the selected weight ratio for the diamines to analyze their properties. It could be observed that this amount could promote the consumption of cyclic carbonates as seen from the FTIR spectra (**Figure 16 c-e**) along with yielding flexible NIPU films used for testing. Based on that, the curing process over time for the EDA, BDA, and HAD-based NIPU is presented in **Figure 16(c-e)**, respectively. Through that, some characteristic peaks could be observed even after short

curing times such as the amide bond stretch (-CONH) at  $1630\text{ cm}^{-1}$ , -C=O ester stretch at  $1700\text{ cm}^{-1}$ , C-N stretch at  $1540\text{ cm}^{-1}$ , N-H and O-H stretches in the range of  $3300\text{-}3440\text{ cm}^{-1}$  [53]. The O-H stretches around  $3500\text{ cm}^{-1}$  could also be observed simultaneously with the N-H as the reaction between the cyclic carbonates and primary amines leads to the formation of OH groups forming hydroxy urethane moieties [43,55,56]. Also, C-O stretch vibrations around  $1170\text{ cm}^{-1}$  could be observed. The presence of OH groups after the reaction between cyclic carbonates and primary amines is one of the aspects that differs the NIPUs from the isocyanate-based PU. It has been reported that when higher ratios of isocyanate are used to react with a polyol, the FTIR spectra of those PUs presented peaks around  $3320\text{ cm}^{-1}$  assigned to N-H stretches as well as peaks around  $2260\text{-}2270\text{ cm}^{-1}$  assigned to unreacted isocyanate groups [57,58].

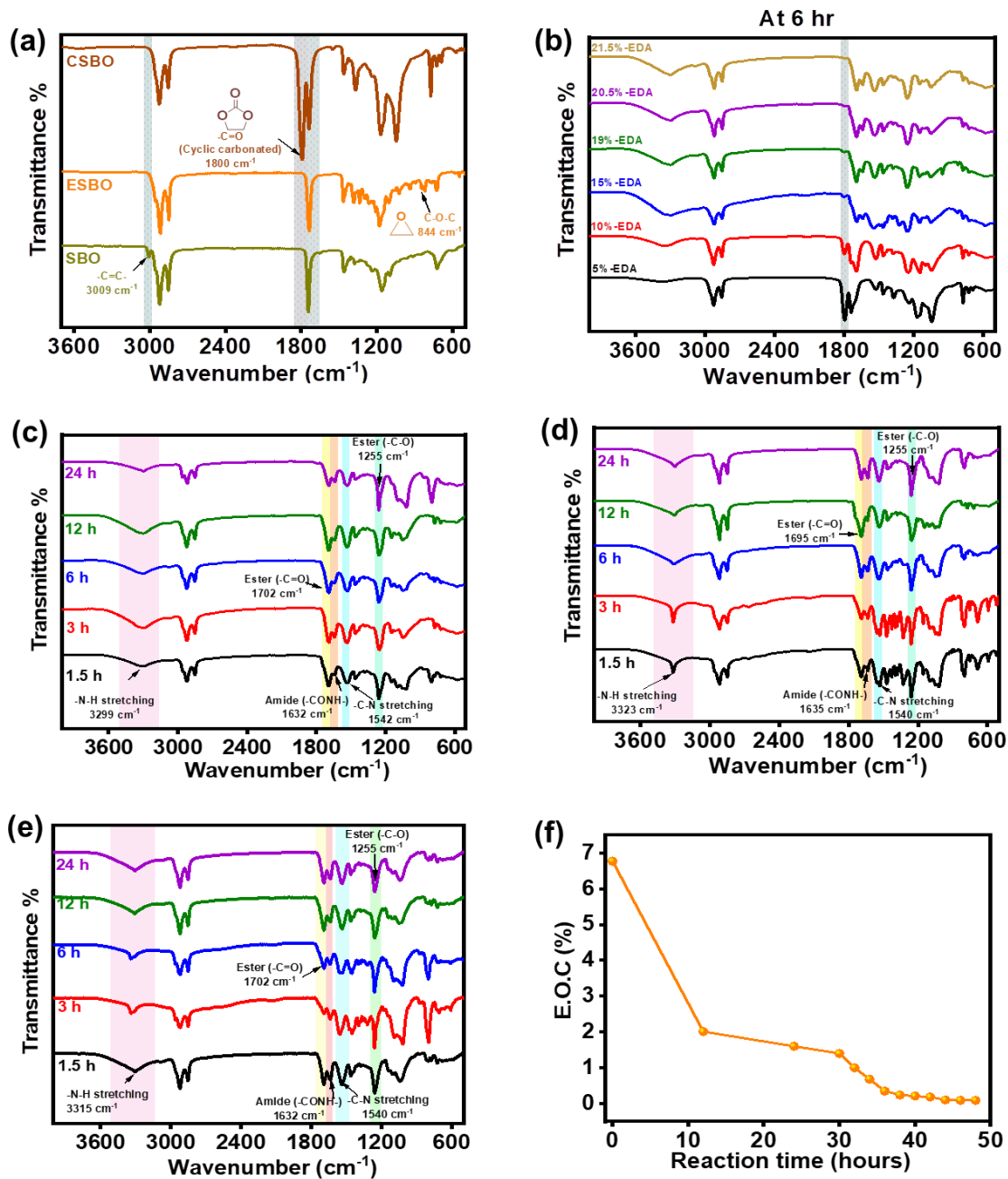


**Figure 16.** FTIR spectra of (a)SBO, ESBO, and CSBO. (b) Different EDA to CSBO weight ratio at 6 hours. FTIR spectra were obtained from the increasing curing time for the NIPUs obtained from (c) EDA, (d) BDA, and (e) HDA (f) Decrease of epoxy concentration as a function of reaction time Decrease of epoxy concentration as a function of reaction time.

### 3.1.2. Gel Permeation Chromatography

The GPC is one of the most utilized techniques as it is a relative method used to determine important aspects of a material such as its molecular weight, and polydispersity index, among others. GPC was performed to confirm the conversion of epoxy groups into cyclic carbonates as presented by the chromatogram of ESBO and CSBO in **Figure 17**. It could be observed that CSBO presented a shorter elution time when compared to ESBO which indicated that it presented higher molecular weight as it could go faster through the column.

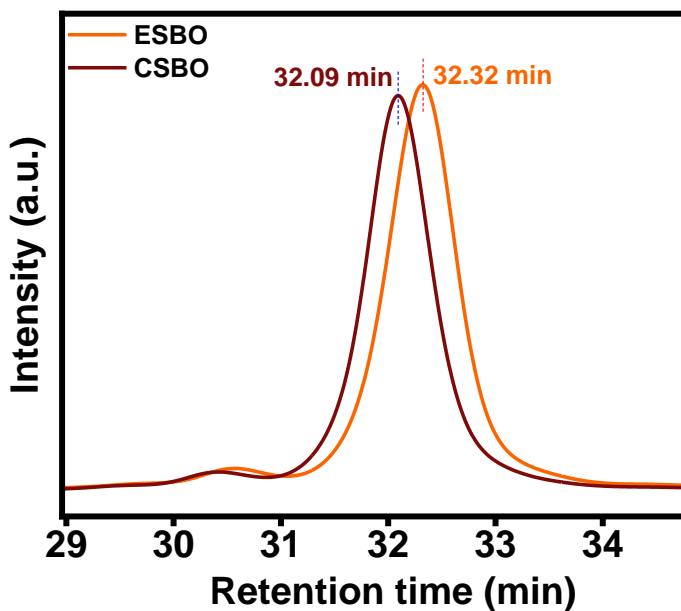


**Figure 17.** GPC of ESBO and CSBO from GPC.

### 3.1.3. Nuclear Magnetic Resonance

The NMR is one of the most important techniques to elucidate the chemical structure of a compound, serving as one of the most important tools in chemistry and

material science. The  $^1\text{H}$  NMR spectra for SBO, ESBO, and CSBO are presented in **Figures 18, 19, and 20**, respectively. The spectra of SBO (**Figure 18**) had the peaks assigned to protons adjacent to the bonded to the C=C and the highly polarized proton bonded to the secondary C-O from the triglyceride there were within the range of 4.9 to 5.3 ppm marked as “a” [59]. The spectra of ESBO (**Figure 19**) showed a peak at around 2.5 to 3.0 ppm marked as “e” that were assigned to the C-H in the  $\alpha$ -position of the epoxy group [53]. The spectra of CSBO (**Figure 20**) showed new peaks around 4.2 to 5.0 ppm that were assigned to the C-H in the  $\alpha$ -position of the cyclic carbonate groups along with the disappearance of the peaks at around 2.5 to 3.0 ppm assigned to the epoxy groups [60]. Based on that, the conversion of epoxy into cyclic carbonate groups could be confirmed based on the shift of these peaks. Based on that, the proposed structures for the NIPU are presented in **Figure 21**.

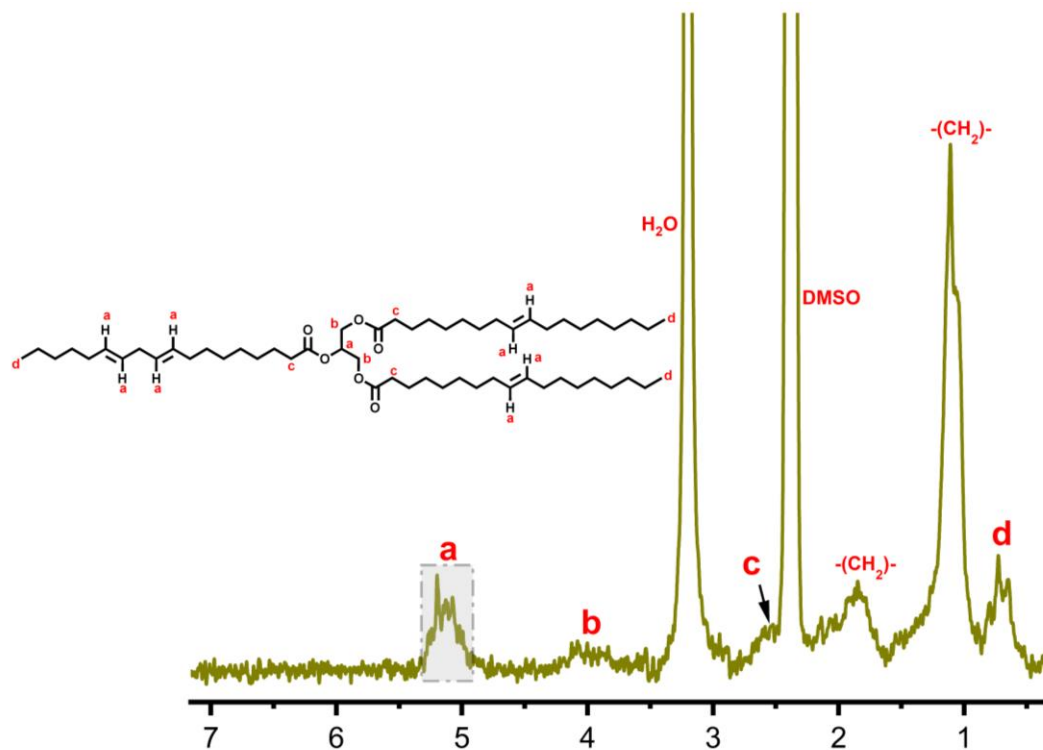


Figure 18. <sup>1</sup>H NMR spectra of SBO.

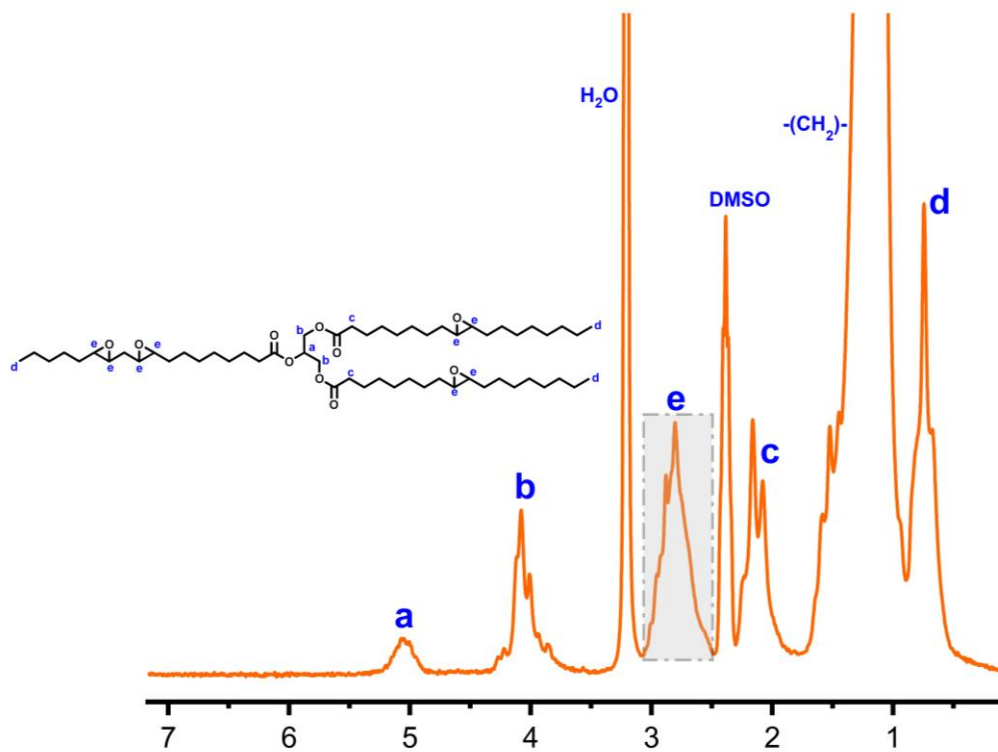
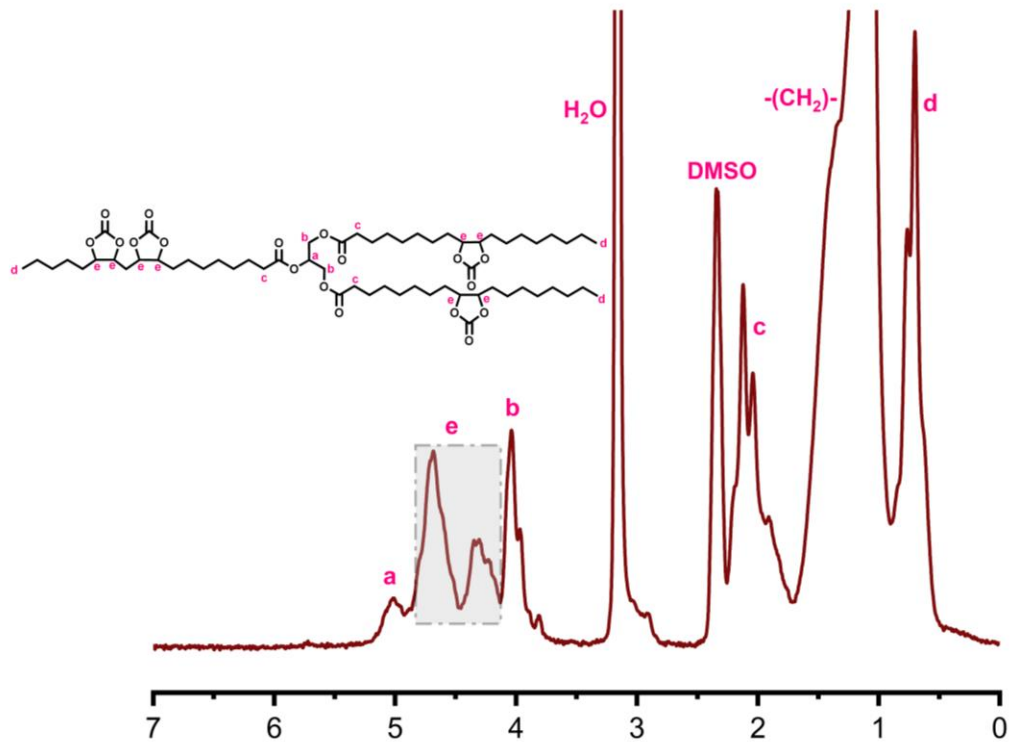
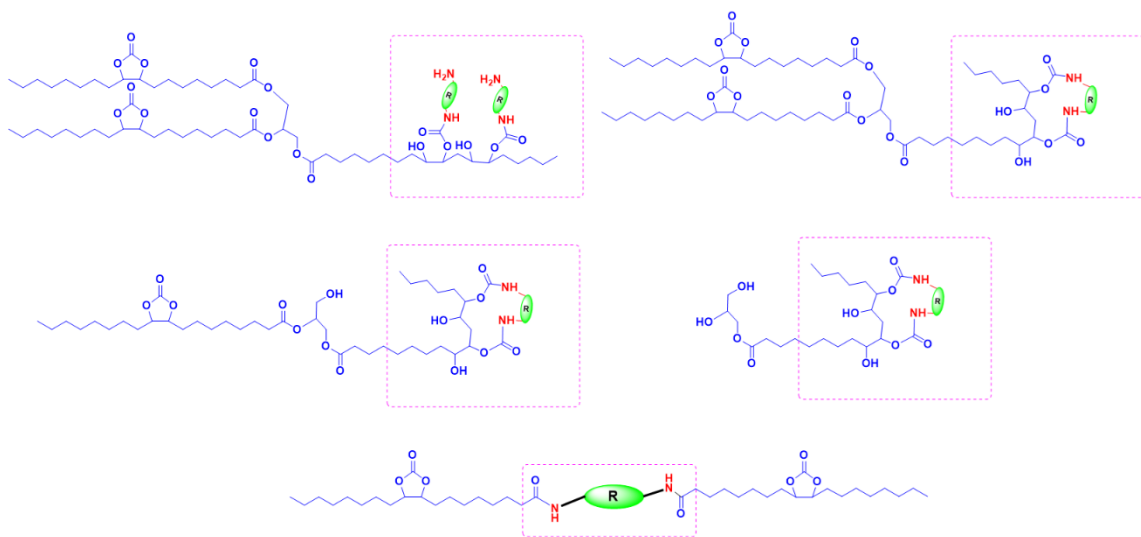


Figure 49. <sup>1</sup>H NMR spectra of ESBO.



**Figure 20.**  $^1\text{H}$  NMR spectra for CSBO.



**Figure 21.** Proposed chemical structures after the reaction between CSBO and a diamine to form the NIPU films.

### 3.2. Thermogravimetric Analysis

The TGA is an important test to understand the thermal properties of a polymer such as working temperature, degradation behavior, and overall thermal stability. In this sense, **Figure 22** shows the TGA and derivative TGA (DTGA) for the NIPU obtained from EDA, BDA, and HDA at increasing curing times. In general, the TGA plots displayed similar degradation profiles. However, some slight differences were observed as presented in **Table 1**. Generally, there was an increase in degradation temperature with a longer curing time. Such results were expected since a shorter curing time would be more likely to present unreacted diamines in the system which degrade at lower temperatures. From that, as presented in **Table 1**, considering the NIPUs cured for 24h, the decomposition temperature at 5% wt. loss ( $T_{d5\%}$ ), decomposition temperature at 50% wt. loss ( $T_{d50\%}$ ), and maximum decomposition temperature ( $T_{max}$ ), determined as the highest peak at the DTGA plot, were progressively higher for BDA-, EDA-, and HDA-based NIPUs. Also, longer aliphatic chains can introduce some improvement in thermal stability, hence the relatively larger aliphatic chain of HDA could have been a factor for higher thermal degradation temperatures when compared to EDA and BDA since there was a larger population of C–C bonds that present a dissociation energy of 359.2 kJ/mol which is higher than C–N 337.7 kJ/mol [61,62]. It could also be observed that, on the DTGA, the NIPU films obtained from EDA presented three distinct peaks. The first peak could be associated with the decomposition of the diamine segment from the structure. Correlated to that, the first decomposition of the BDA- and HDA-containing NIPUs occurred at higher temperatures which could be due to the higher dissociation energy of C–C bonds that are present in a larger population in HDA and BDA in comparison to EDA. The second decomposition

temperature could be attributed to the polymer's backbone chain. Yet, in the case of BDA- and HDA-containing NIPUs the first and the second thermal decompositions could have occurred simultaneously due to the higher temperatures required for the degradation of BDA and HDA. This thermal behavior was similar to a previous report from Xin He [61].

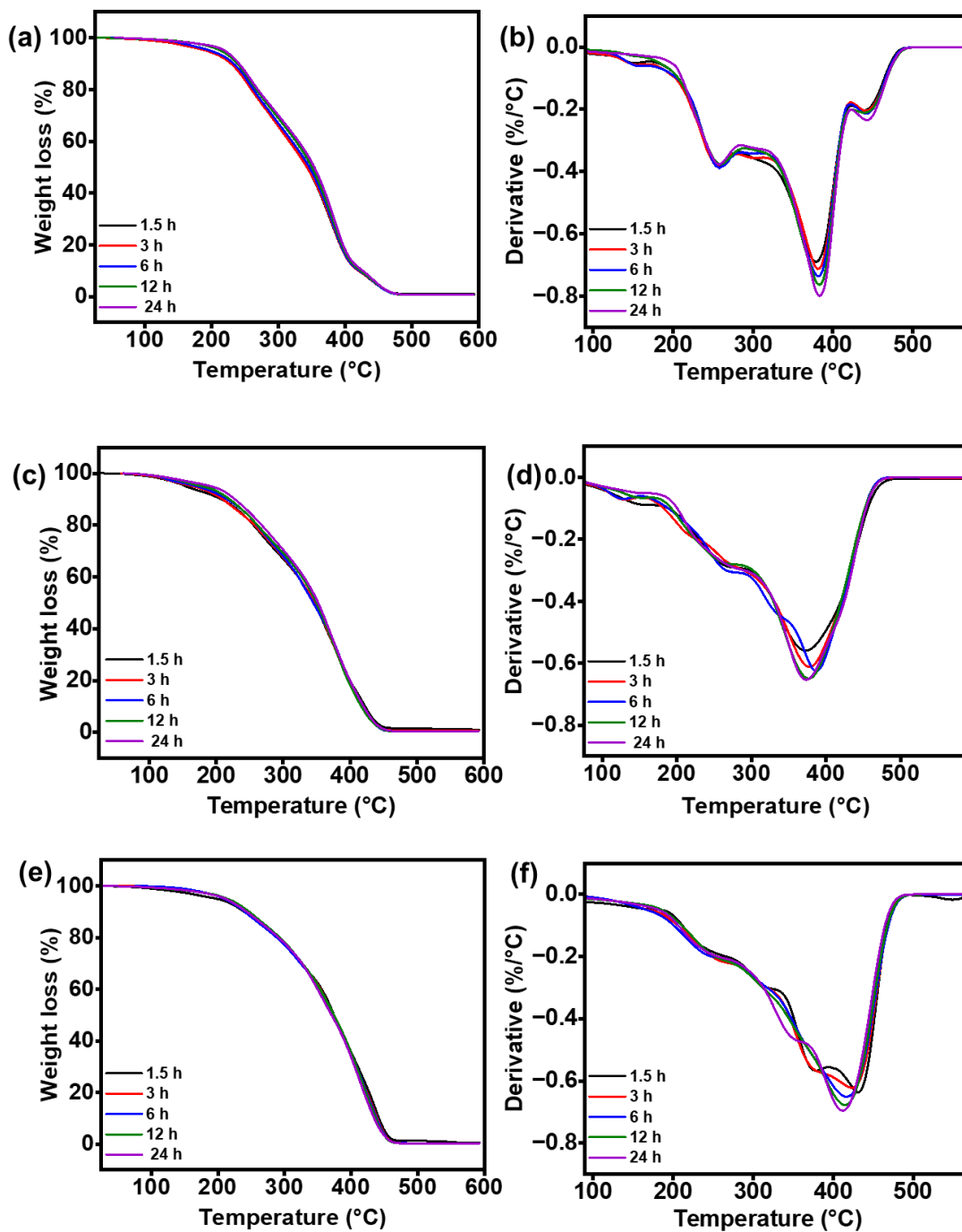


**Figure 22.** TGA and DTGA plots for the NIPU films cured at different times were obtained from the diamines (a, b) EDA, (c, d) BDA, and (e, f) HDA.

**Table 1.** Decomposition temperatures for the NIPU containing EDA, BDA, and HDA.

<b>Diamine</b>	<b>Curing Time (h)</b>	<b>Td<sub>5%</sub> (°C)</b>	<b>Td<sub>50%</sub> (°C)</b>	<b>T<sub>max</sub> (°C)</b>	<b>Residue at 600 °C (%)</b>
<b>EDA</b>	1.5	197	342.92	378.09	0.861
	3	192	342.36	381.74	0.578
	6	198	345.93	379.65	0.624
	12	214	349.79	384.54	0.608
	24	219	353.42	383.57	0.706
<b>BDA</b>	1.5	154	346.63	372.88	0.987
	3	166	346.92	377.76	0.561
	6	171	345.1	387.11	0.444
	12	179	349.92	376.98	0.383
	24	192	352.31	375.34	0.396
<b>HDA</b>	1.5	199	374.34	431.25	0.509
	3	211	372.79	423.53	0.304
	6	209	373.54	416.93	0.33
	12	214	374.26	415.02	0.322
	24	211	370.66	412.5	0.287

### 3.3. Differential Scanning Calorimetry

The DSC is a valuable tool to elucidate the thermal transitions of a polymer in a controlled environment. Under this line, **Figure 23** displays the DSC plots for EDA, BDA, and HDA-based NIPUs, respectively. Generally, it could be observed that the glass

transition temperature ( $T_g$ ) tended to increase with the curing time. Such behavior was expected since the amine groups would have more favorable conditions to react with the CSBO likely leading to longer polymeric chains that could be more entangled and, therefore, promote an increase in the  $T_g$ . However, both EDA and BDA displayed at least two thermal transitions regardless of the curing time. These thermal transitions could be, perhaps, associated with the different mobilities of urethane and amide linkages as it could be possible that both moieties are present in the polymeric structure of the film as backed by FTIR. In addition, EDA and BDA are generally more reactive than HDA which could suggest that the former two were less selective to react with either the carbonyl from the ester bond inherently present in the vegetable oil that would lead to an amide or the carbonyl from the cyclic carbonate group that would lead to a urethane group [53]. Also, as the aliphatic chain size of the diamines increased there was a slight increase in the  $T_g$  range as EDA, BDA, and HDA-based NIPUs presented values from -25 to -20 °C, -10 to 0 °C, and 5 to 10 °C, respectively. This range of values was similar to previously reported studies on NIPUs [40,61].

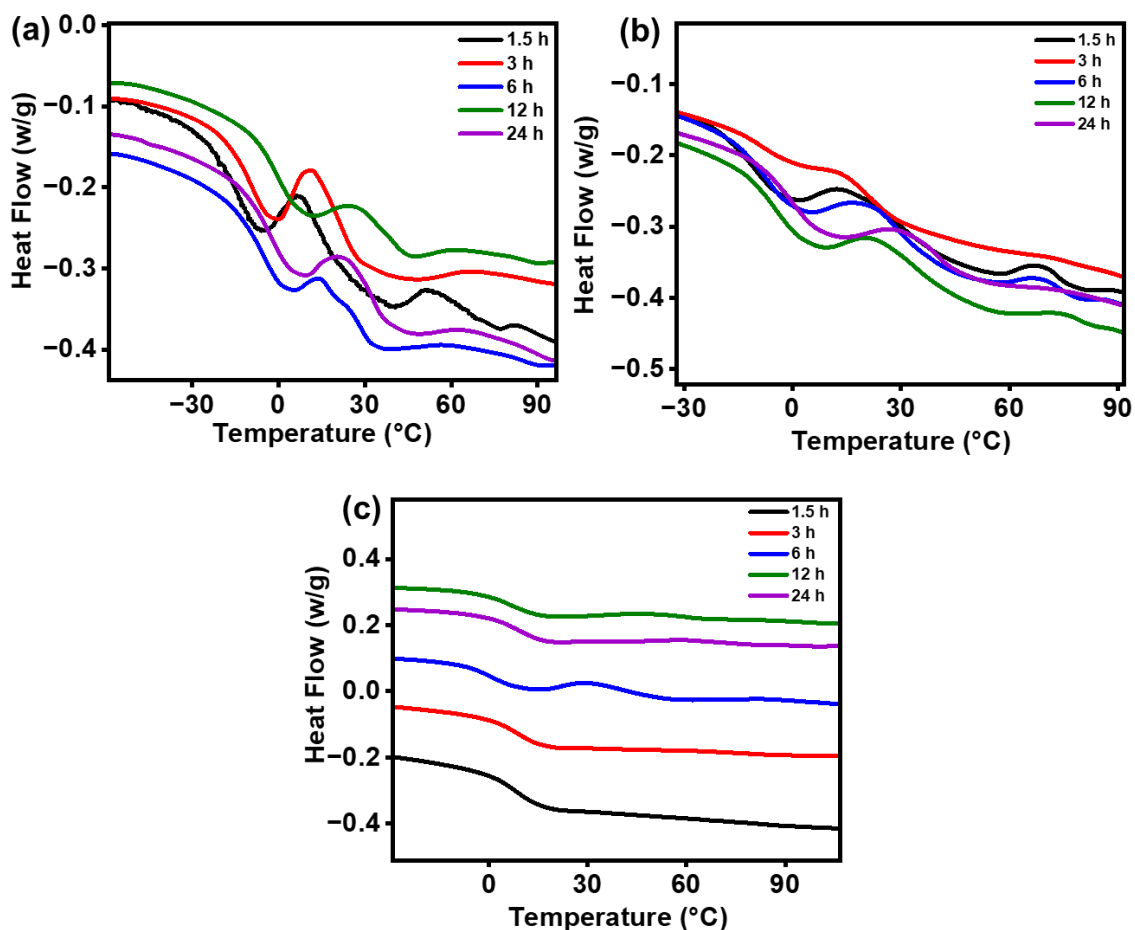


**Figure 23.** DSC for the NIPU films based on (a) EDA, (b) BDA, and (c) HDA.

Further on, the comparison of EDA-, BDA-, and HDA-based NIPU at the same curing time of 1.5, 3, 6, 12, and 24h are shown in **Figure 24**. It could be observed that both BDA and EDA-based NIPUs presented multiple thermal transitions at shorter curing times whereas HDA-based NIPU presented two which, as previously mentioned, could be associated with the transition temperatures associated with the amide and the urethane segments.

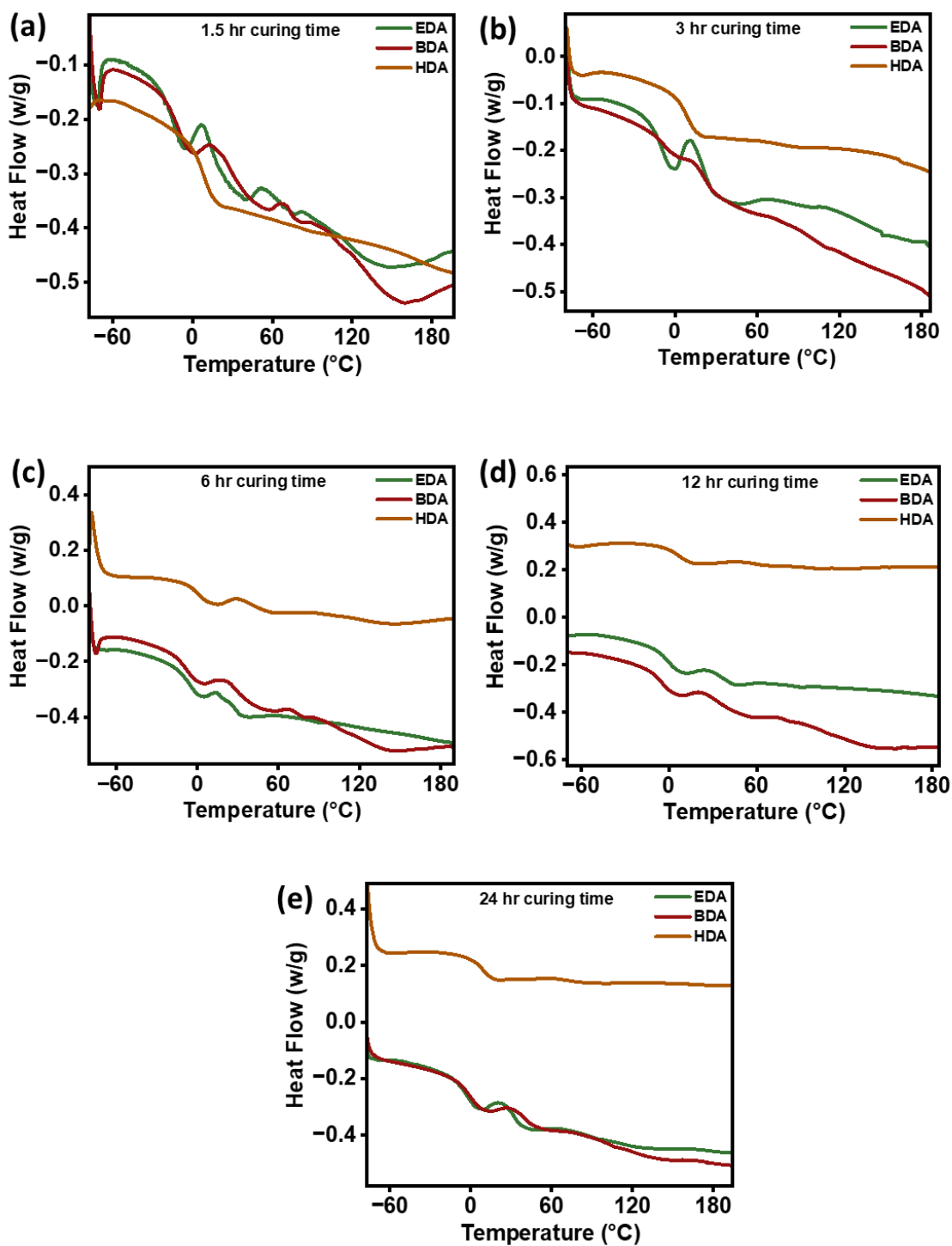


**Figure 24.** DSC thermograms for the EDA-, BDA-, and HDA-based NIPU films at increasing curing times of (a) 1.5h, (b) 3h, (c) 6h, (d) 12h, (e) 24h.

### 3.4. Dynamic Mechanical Analysis

The DMA is a versatile technique that can be used to elucidate some of the thermal and mechanical properties of a material under specific conditions such as varying dynamic forces in function of temperature. From that, valuable information can be obtained regarding the viscoelastic behavior of the material. The DMA analysis of the NIPU containing EDA, BDA, and HDA is presented in **Figures 25, 26, and 27**. The compiled information for DSC and DMA is presented in **Table 2**. It was notable from the DMA plots for EDA-, BDA-, and HDA-based NIPUs, that at short curing times, there were two distinct peaks for the Tan delta for the NIPU films whereas at longer curing times the two peaks tended to merge. Based on that, it could be proposed that the short curing time could have prevented some of the reactions of the diamines with the cyclic carbonates, which was more likely to result in a shorter polymeric chain with a lower degree of crosslinking [40]. Taking the information from FTIR, it was observed that regardless of the curing times moieties such as carbonyl and amines were observed which could suggest the presence of both urethanes and amides in the NIPUs. Yet, at shorter curing times, the NIPUs presented more separated tan delta peaks which suggested the occurrence of two  $T_g$  processes. Perhaps, one could be attributed to the  $T_g$  of chains formed from the reaction of diamines with cyclic carbonates that resulted in urethanes, whereas the other could be related to the reaction of diamines with the carbonyl esters derived from the triglycerides in the vegetable oil's structure that led to the formation of amides. At longer curing times, it could be observed an approximation of the peaks. Such an effect could be due to the longer time that allowed the diamines or end-reactive groups to react, leading to polymeric chains containing both urethanes and amide groups.

Further on, it could be observed that there was a decreasing value of  $T_g$  from the order EDA, BDA, and HDA-based NIPUs as shown in **Table 2**. It could be proposed that the shorter aliphatic chain of EDA- led to the formation of less spaced rigid and polarized segments that could present more hydrogen-bonding interactions when compared to BDA- and HDA-based NIPUs that presented slightly longer aliphatic chains that displayed weaker intermolecular interactions. Because of that, the EDA-based NIPU was more likely to present higher temperatures to disrupt these intermolecular interactions to allow the polymeric chains to move. Hence, higher  $T_g$  values. In addition to that, the decrease in the trend in the decrease of  $T_g$  could be attributed to the reduction of the content of amine groups at a fixed concentration of carbonate moieties, which could have led to a decrease in the crosslinking density of the NIPU. Such a condition facilitates the movement of polymeric chains, causing the  $T_g$  to decrease.

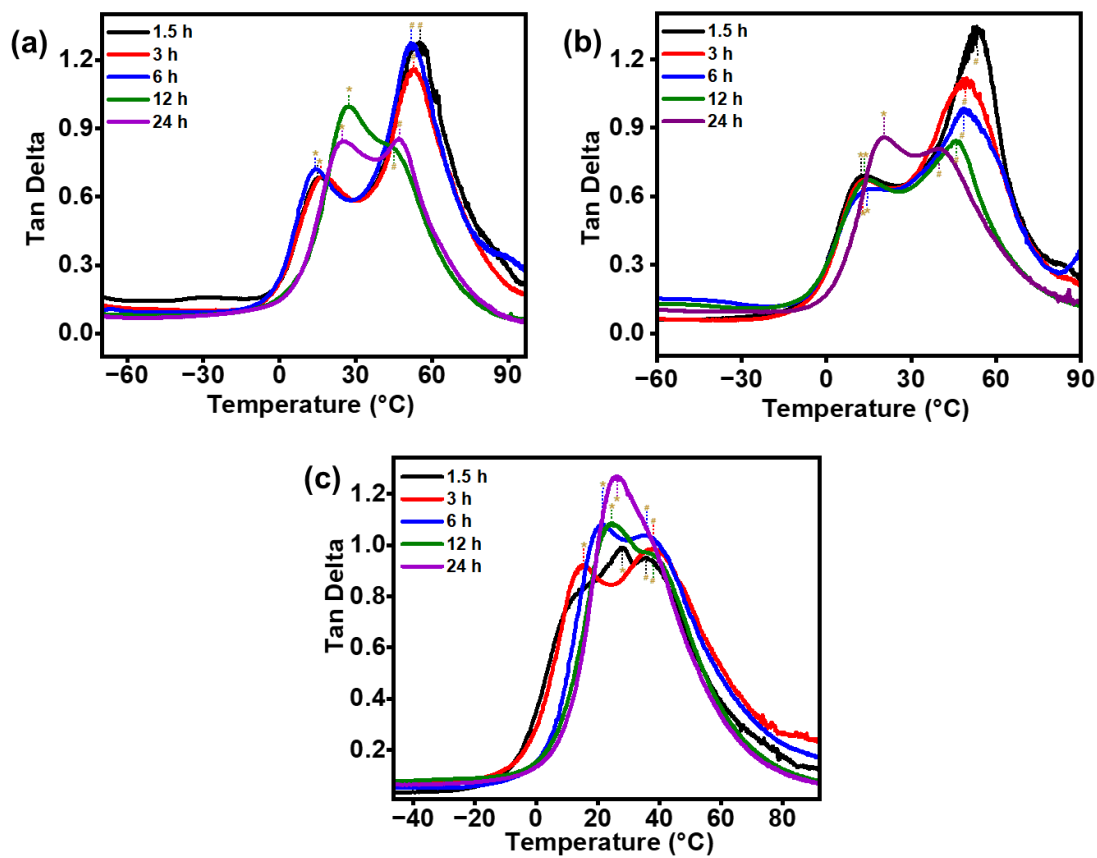


**Figure 25.** DMA plots for EDA, BDA, and HDA-based NIPU films, respectively, for (a-  
c) tan delta

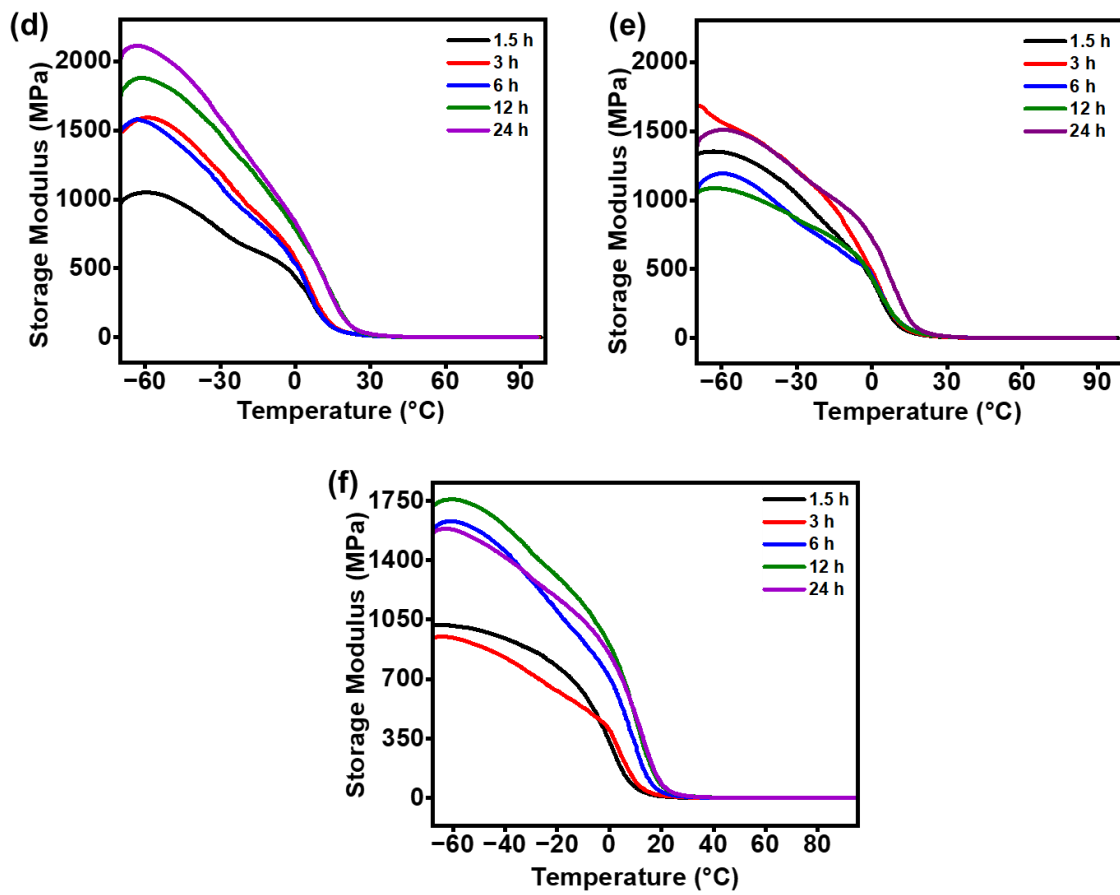


**Figure 26.** DMA plots for EDA, BDA, and HDA-based NIPU films, respectively, for (a-  
c) storage modulus

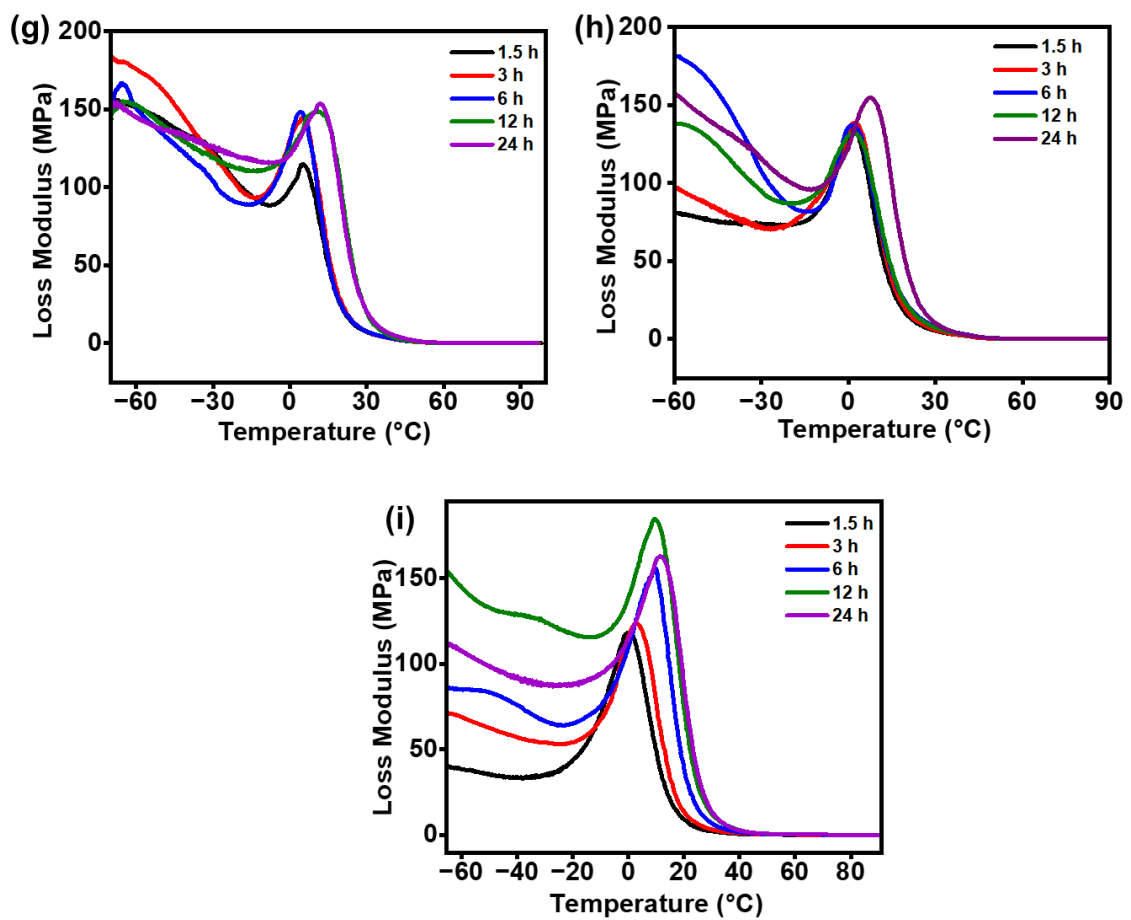


**Figure 27.** DMA plots for EDA, BDA, and HDA-based NIPU films, respectively, for (a-  
c) loss modulus.

**Table 2.** Transition temperatures for the NIPU containing EDA, BDA, and HDA for DSC and DMA.

<b>Diamine</b>	<b>Curing Time (h)</b>	<b>T<sub>g</sub> DSC (°C)</b>	<b>T<sub>g</sub> DMA (°C)</b>
<b>EDA</b>	1.5	15.27	55.28
	3	16.07	52.75
	6	14.04	52.22
	12	26.92	44.90
	24	24.79	47.08
<b>BDA</b>	1.5	12.74	52.77
	3	12.97	48.95
	6	14.23	48.69
	12	13.42	45.93
	24	20.25	39.80
<b>HDA</b>	1.5	27.80	35.72
	3	15.18	37.74
	6	21.58	35.18
	12	24.62	37.64
	24	25.90	-

### 3.5. Hardness and Tensile Strength

The mechanical properties of the NIPU films obtained through the curing process with different diamines were evaluated. **Figure 28(a)** displayed the Shore D hardness of the EDA, BDA, and HDA-based NIPUs at different curing times. It could be observed that

all the NIPU films presented an increase in hardness with an increasing curing time. Such an effect was expected as longer curing times promoted the reaction of the diamines with the cyclic carbonate moieties which could lead to an increase in molecular weight, cross-linking density, and hydrogen bonding in the NIPU backbone. Such factors are likely to increase the hardness of a polymeric film. After 24h of curing process the EDA, BDA, and HDA-based NIPUs presented a Shore D hardness of around 20, 18, and 22, respectively. The highest hardness for the HDA-based NIPU could be perhaps attributed to a larger polymeric chain entanglement given that the slightly larger aliphatic chain of HDA could promote an increase in the hardness of the NIPU.

The tensile strength of the NIPU films is presented in **Figure 28(b)**. It could be observed that longer curing times led to an increase in tensile strength. From that, the highest values were obtained for the NIPU films cured at 24h which were around 2.7, 0.7, and 0.5 MPa for EDA, BDA, and HDA-based NIPU films, respectively. The higher tensile strength observed for the EDA-based NIPU film could be attributed to the smaller aliphatic chain of the EDA that led to a higher degree of crosslinking that was likely to make the NIPU structure more densely packed as shown in **Figure 29**. Because of that, the polymeric structure of EDA-based NIPU required a larger amount of force to enable its movement as it presented slightly smaller aliphatic chains that are less flexible than the ones of BDA and HDA-based NIPU, which resulted in higher tensile strength. The NIPU film's flexibility during the tensile test is shown in **Figure 28(c)**. The general flexibility of the NIPU-based films in terms of stretching, twisting, folding, and wrapping is presented in **Figure 28(d)** as well and the NIPU film specimen that was cast in a mold to attain the bone shape to be used for tensile testing is presented in **Figure 28(e)**. The plots of stress vs strain

demonstrated that increasing curing times led to an overall increase in tensile stress accompanied by a decrease in strain. Based on that, it could be proposed that there was an increase in crosslinking degree at longer curing times which led to a more brittle film resulting in higher tensile strengths with lower elongations. Yet, HDA-based NIPU film cured for 24h displayed appreciable mechanical properties by presenting an elongation of around 2% and a stress of around 0.5 MPa. Based on that, it could be proposed that the curing time promoted some degree of crosslinking that influenced the tensile stress whereas the longer aliphatic chain of HDA introduced some degree of flexibility on the chains. Further on that, the Young's Modulus (MPa) which is the slope of the gradient of stress/gradient of strain in each range of elongation within the elastic region such as from 0.02% to 0.3% which are displayed in **Table 3**. It could be observed that the EDA-based NIPU displayed the highest Young's Modulus at the elongation for the elongation strain from 0.02% to 0.3% with the value of 3.64 MPa whereas BDA- and HDA-based NIPU presented 0.9925 and 0.4878 MPa, respectively. This data suggested that EDA-based NIPU was stiffer than the other NIPU films likely due to the smaller aliphatic chain that hindered the mobility of the polymeric chains, making it more brittle in comparison to the others.

Some of the mechanical properties of the NIPU films were comparable or higher than the results reported in previous studies on NIPU films [63–65].

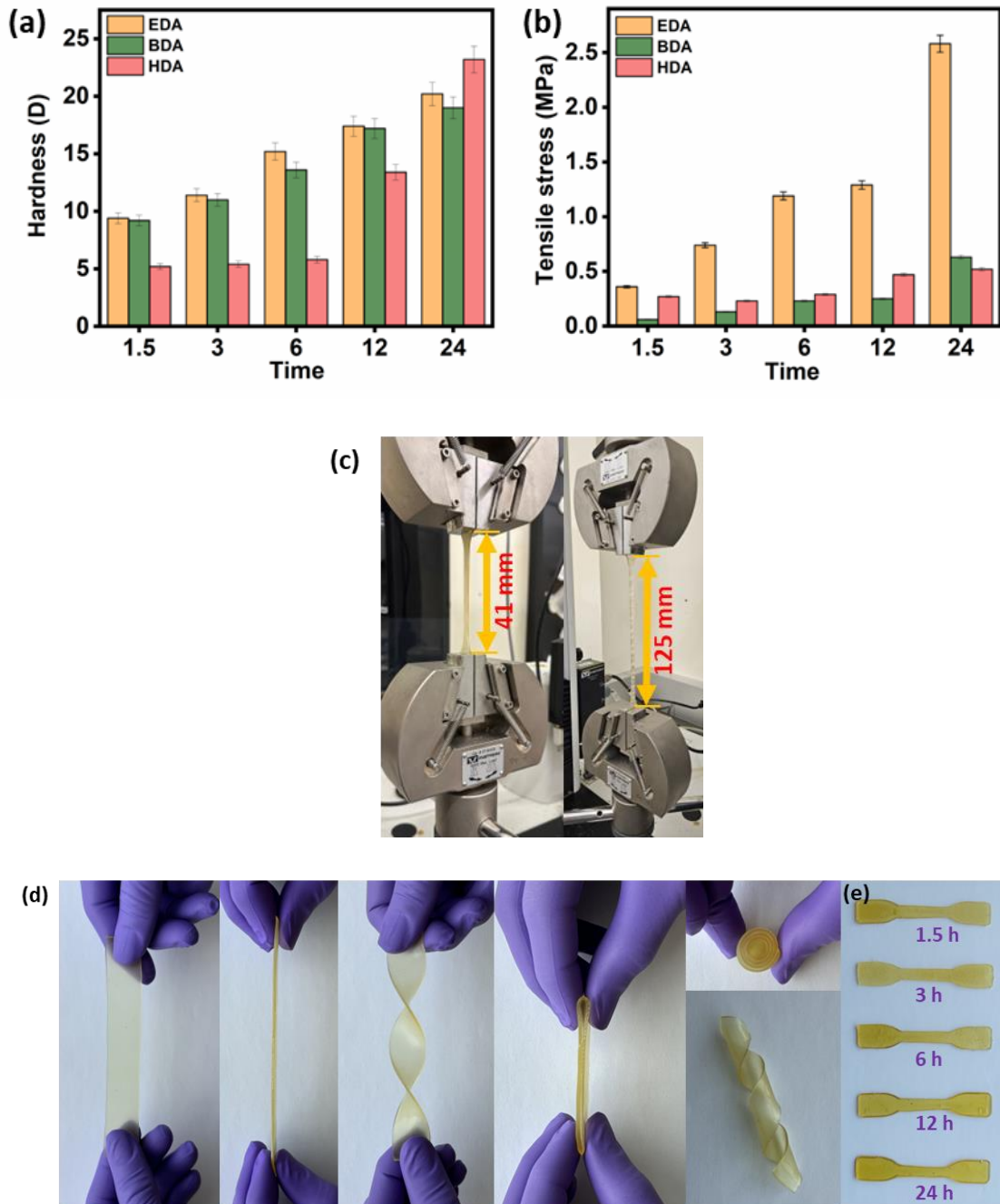


**Figure 28.** (a) Hardness Shore D, (b) tensile strength tests for the NIPU films, (c) Stretchability of the NIPU films during tensile testing, (d) Various aspects of the NIPU film's flexibility, (e) Bone-shaped specimen used for the tensile test.

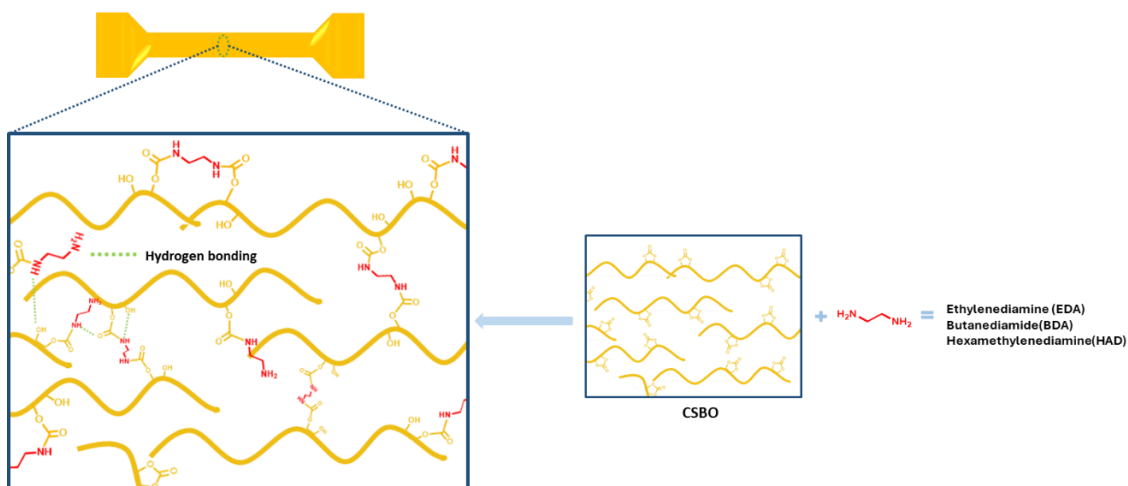


**Figure 29.** Proposed cross-linking structure of urethane bond.

**Table 3.** Young's Modulus (E) for the NIPU films obtained from different diamines with 24 h curing time.

Diamine-based NIPU	Young's Modulus - E (MPa)	Tensile Stress ( $\sigma$ ) (MPa)	Tensile Strain ( $\epsilon$ ) (%)
<b>EDA</b>	3.64	1.97	0.3
		0.95	0.02
<b>BDA</b>	0.99	0.591	0.3
		0.3131	0.02
<b>HDA</b>	0.49	0.2171	0.3
		0.0805	0.02

### 3.6. Degree of Swelling and Gel Content

The degree of swelling (DS) provides some information regarding a polymer's capability to absorb and retain a solvent, whereas the gel content (GC) is the insoluble

fraction of a crosslinked polymer. Hence, the higher the DS, the higher the affinity of the polymer with the solvent, and the higher the GC, the higher the degree of crosslinking. To perform the test, the NIPU films were immersed in dimethyl sulfoxide (DMSO), N-methyl-2-pyrrolidone (NMP), dimethylformamide (DMF), and toluene for 24h. After that, the samples were dried in a vacuum oven at 75 °C for 48h. The swelling capability of the polymer is intrinsically related to its crosslinking degree and its interaction with a given solvent. In this sense, attractive interactions between a crosslinked polymer with solvent lead to a higher degree of swelling. The degree swelling can be calculated through **Equation 3**.

$$DS (\%) = \frac{m_1 - m_0}{m_0} \times 100 \quad (3)$$

Where  $m_0$  is the initial weight and  $m_1$  is the weight after swelling. Yet, a fraction of the polymer itself is dissolved which is removed from the polymer structure upon drying. That condition leads to a reduction of the polymer's weight in comparison to the initial weight of the polymer before swelling which allows the calculation of gel content through **Equation 4**.

$$GC (\%) = \frac{m_2}{m_0} \times 100 \quad (4)$$

Where  $m_2$  is the weight after drying. **Figure 30(a-d)** displays the degree of swelling for the NIPU films at different curing times after their immersion in solvents such as DMSO, NMP, DMF, and Toluene, respectively. In general, it could be observed that EDA-

based NIPU films presented the highest swelling degree in every solvent when compared to both BDA- and HDA-based NIPU films. The order of solvents that promoted the highest degree of swelling were NMP, DMF, DMSO, and toluene. Also, generally, with the increase in curing time, there was a decrease in the swelling degree. Alongside these general aspects that were observed, the HDA-based NIPU film presented the overall lowest degree of swelling. Such phenomena could be attributed to a slightly larger chain entanglement of the polymeric chains from the NIPU obtained from HDA that could limit the gradient of solvent that was absorbed by the polymeric matrix [66].

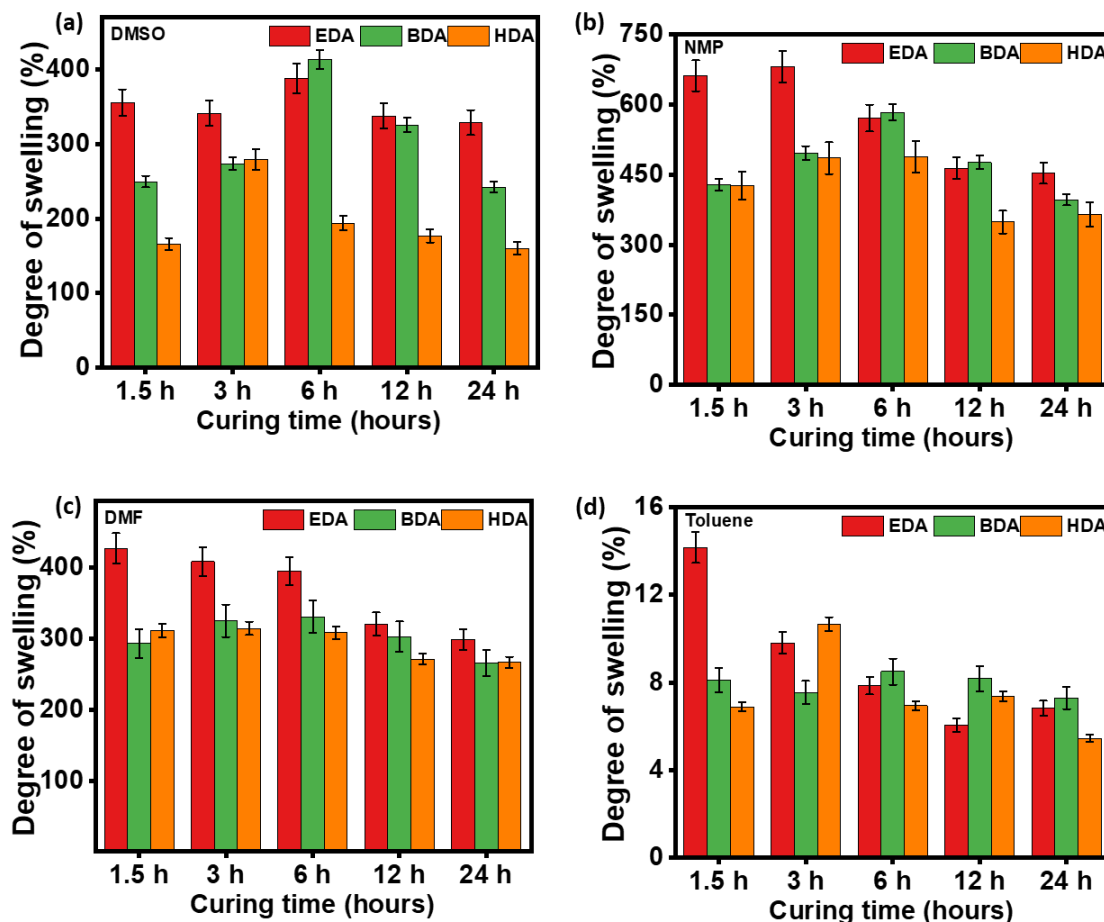


**Figure 30.** Degree of swelling for the NIPU films at increasing curing times at (a) DMSO, (b) NMP, (c) DMF, and (d) toluene.

After the swelling test, the NIPU films were dried for 48h at 75 °C. The final weight of the NIPU films after drying can provide some information regarding the gel content of the polymers as it can be defined as the amount of insoluble fraction of the crosslinked polymer. The gel content for the NIPU films after drying from different solvents DMSO, NMP, DMF, and toluene is shown in **Figure 31(a-d)**, respectively. It could be observed that DMSO, NMP, and DMF could dissolve a larger fraction of the polymeric chain within the network structure due to the general decrease in the gel content of the NIPU films. On the other hand, toluene presented a considerable solubility of the NIPU polymeric chains. Also, similarly to the degree of swelling, the gel content tended to increase with the increase in curing time for all the NIPU films. Based on that, taking into consideration the NIPU films cured at 24h it could be observed that the lowest gel content was around 85% which suggested a satisfactory crosslinking degree for the NIPU films. Further on that, the HDA-based NIPU presented the highest gel content suggesting that most of its structure was crosslinked. On the other hand, the EDA-based NIPU presented the overall lowest gel content which suggested that it presented a considerable amount of soluble polymeric chains that could be extracted from the network upon drying. The physical aspects of the NIPU films after drying are presented in **Figure 32**.

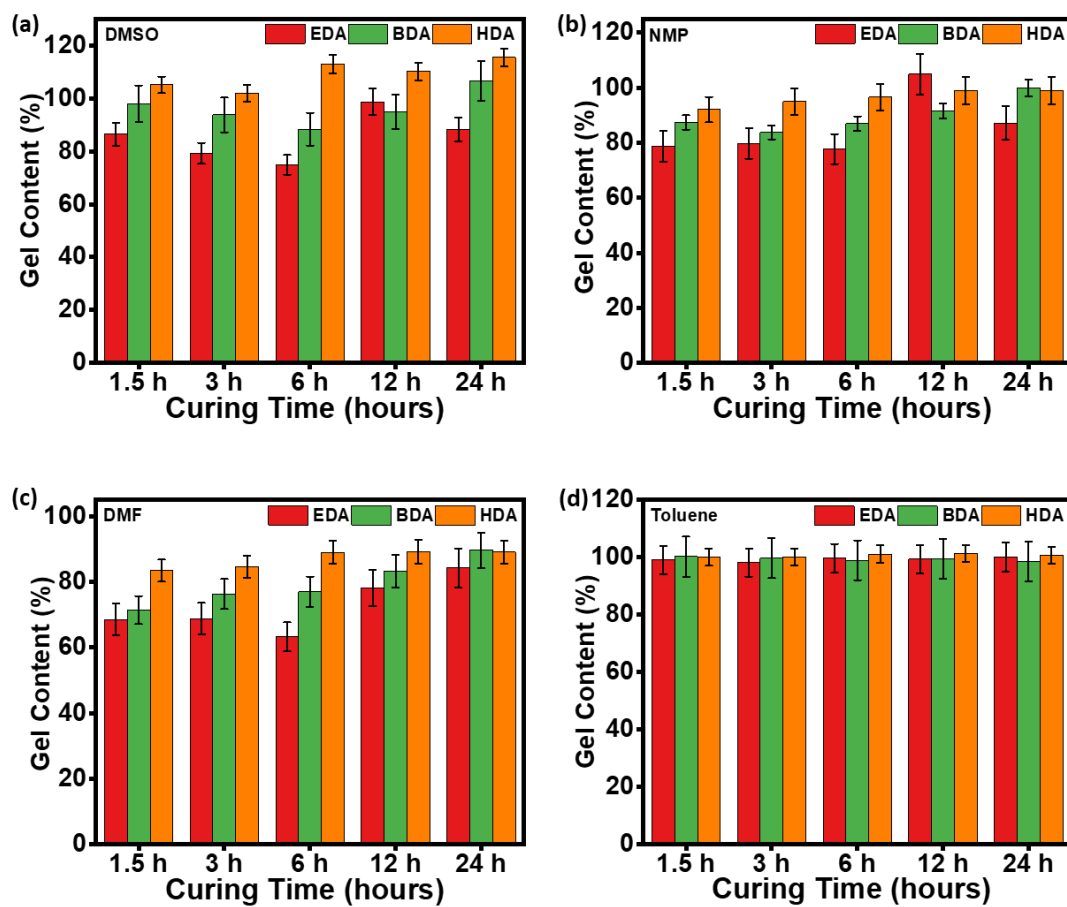


**Figure 31.** Gel content for the NIPU films at increasing curing times at (a) DMSO, (b) NMP, (c) DMF, and (d) toluene.

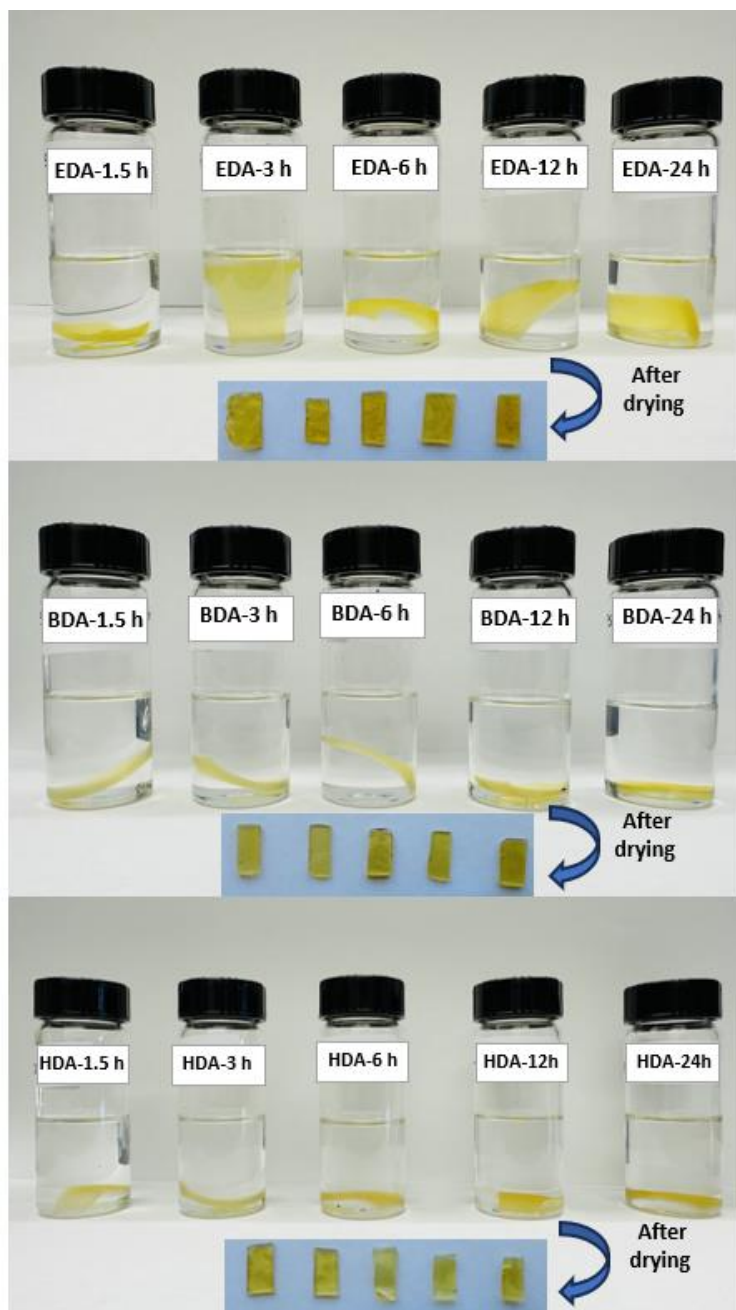
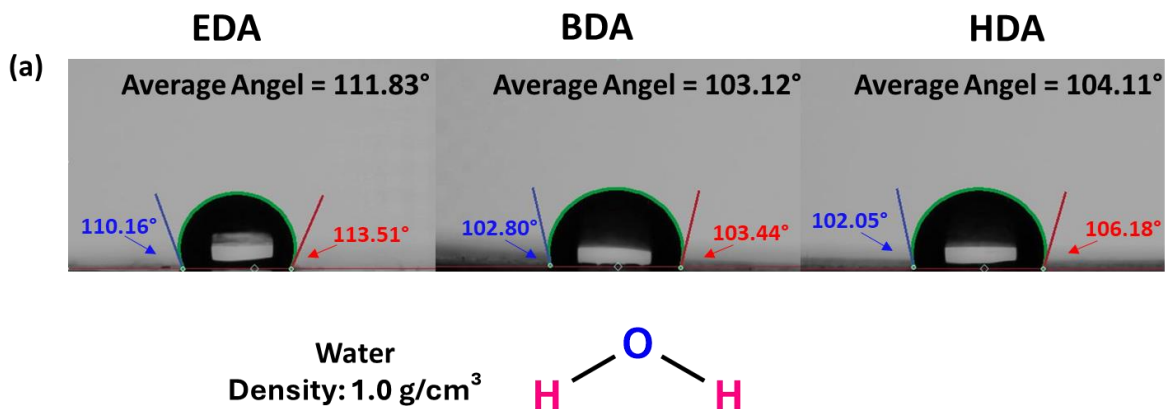


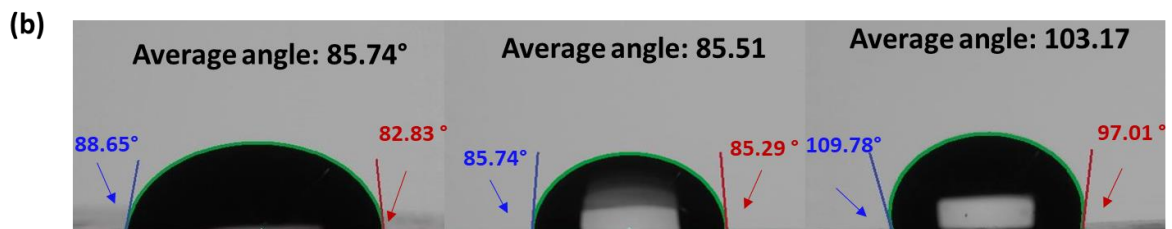
**Figure 32.** The physical aspect of the swollen NIPU films after drying.

### 3.7. Contact Angle Measurement

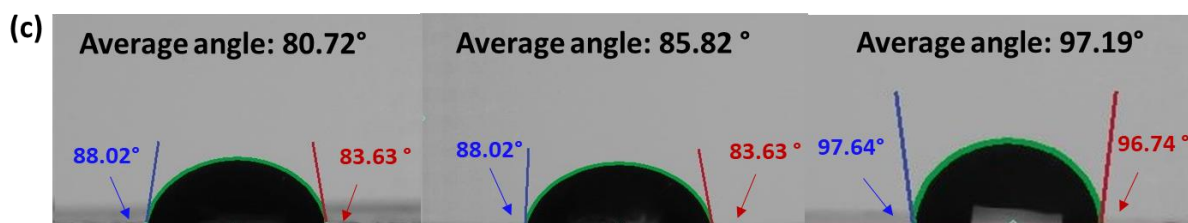
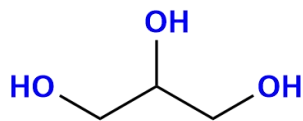
The contact angles for the NIPU films were performed in several solvents such as water, glycerol, ethylene glycol, dimethyl sulfoxide, and dimethyl formamide which are

shown in **Figure 33 (a-e)**, respectively. For the case of water (**Figure 33 a**) the average contact angles for EDA-, BDA-, and HDA-based NIPU films were 111.83°, 103.12°, and 104.11°, respectively. It was observed that the films presented relatively similar contact angles with values above 90° which can characterize them as hydrophobic. Yet, upon decreasing the polarity of the solvents in the order of glycerol (**Figure 33 b**), ethylene glycol (**Figure 33 c**), dimethyl sulfoxide (**Figure 33 d**), and dimethyl formamide (**Figure 33 e**) there was an overall decrease in the contact angle which reinforced the hydrophobic behavior of the NIPU films. Yet, generally, the HDA-based NIPU film presented the highest contact angles in comparison to EDA- and BDA-based NIPU films, except for the case of dimethyl formamide. Based on that, it could be proposed that the longer aliphatic chains of HDA led to a general increase in contact angle, suggesting that it tended to repel the solvents in comparison to EDA- and BDA-based NIPU films. Yet, HDA-based NIPU film had a stronger interaction with a non-polar solvent such as dimethyl formamide as compared to the other solvents which led to a lower contact angle. Based on that, in general, the films presented a hydrophobic nature.

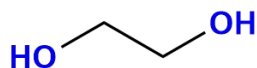




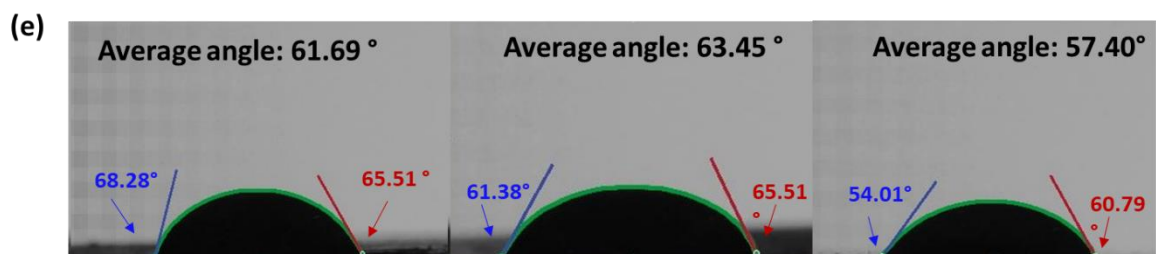
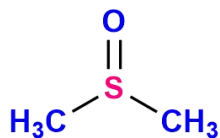
Glycerol  
Density: 1.26 g/cm<sup>3</sup>



Ethylene glycol  
Density: 1.11 g/cm<sup>3</sup>



Dimethyl sulfoxide  
Density: 1.1 g/cm<sup>3</sup>



Dimethyl formamide  
Density: 0.944 g/cm<sup>3</sup>

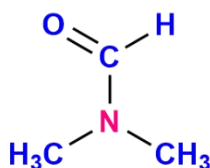


**Figure 33.** Contact angles for the 24h cured EDA-, BDA-, and HDA-based NIPU films in for (a) water, (b) glycerol, (c) ethylene glycol, (d) dimethyl sulfoxide, and (e) dimethyl formamide.

## **CHAPTER IV**

### **CONCLUSION**

In conclusion, this paper described a feasible approach to obtain NIPU films using CSBO that were polymerized with the use of different diamines with increasing sizes of their aliphatic chains. The solvent- and catalyst-free procedure along with a straightforward film casting technique to obtain the NIPU film can make the scalability of these polymeric materials more feasible. On top of that, the isocyanate-free and use of bio-based starting materials such as SBO account for an eco-friendly credential for the NIPU. This study revealed that through the control of simple variables such as type of diamine and curing time, the films can cover a wide range of mechanical properties as they went for relatively brittle and rigid, as for the case of EDA-based NIPU, to gradually more elastic and flexible as for the case of BDA- and HDA-based NIPUs. Following that, it was observed that curing time held the most detrimental effect on overall properties leading to a general improvement in thermal decomposition, hardness, tensile strength, and reduction in the degree of swelling. On the other hand, an increase in the size of the aliphatic chains of the diamines i.e., EDA, BDA, and HDA, led to an increase in thermal decomposition and a decrease of hardness, tensile stress, and degree of swelling. In terms of mechanical properties, it was notable that, with the increase of the aliphatic chain size of the diamines there was a shift towards tougher NIPU films which could be relatively more elastic while

withstanding higher stress values as for the case of HDA-based NIPU. Based on these findings, the NIPU films obtained in this work help in the elucidation of the structure-property relationship along with providing a facile approach for the fabrication of polymeric materials with sustainable and eco-friendly aspects.

## **CHAPTER V**

### **FUTURE WORK**

NIPU represents a compelling avenue for research and development in polymer science, offering solutions to environmental and health challenges linked with conventional isocyanate-based polyurethanes. The above work is based on the aliphatic chain length study which provides flexible material. In the future, another approach will gain attention as researchers incorporate aromatic building blocks into NIPU formulations. Aromatic building blocks will be expected to offer enhanced hardness and strength compared to their aliphatic counterparts. This advancement will enable the development of NIPU materials with superior mechanical properties, making them well-suited for a wider range of applications that require toughness and durability. Furthermore, NIPU materials, with their inherent sticky nature and isocyanate-free bonding method, are poised to attract the attention of the adhesive industry. This eco-friendly approach offers a small yet significant step towards environmental sustainability.

## REFERENCES

- [1] Y. Yanping, The development of polyurethane, *Mater. Sci. Mater. Rev.* 1 (2018) 1–8.
- [2] R.K. Gupta, A.K. Mishra, eds., *Eco-Friendly Waterborne Polyurethanes*, 1st ed., Boca Raton, FL, 2022.
- [3] R.K. Gupta, P.K. Kahol, eds., *Polyurethane Chemistry: Renewable Polyols and Isocyanates*, 1st ed., American Chemical Society, Washington, DC, 2021.
- [4] U. Šebenik, M. Krajnc, Influence of the soft segment length and content on the synthesis and properties of isocyanate-terminated urethane prepolymers, *Int. J. Adhes. Adhes.* 27 (2007) 527–535.
- [5] K.B.H. Badri, W.C. Sien, M.S.B.R. Shahrom, L.C. Hao, N.Y. Baderuliksani, N.R. Adawiyah Norzali, *FTIR Spectroscopy Analysis of the Prepolymerization of Palm-Base Polyurethane*, *Solid State Sci. Technol.* 18 (2010) 1–8.
- [6] U. Panchal, M.L. Chaudhary, P. Patel, J. Patel, R.K. Gupta, *Soybean-Based Bio-Adhesives: Role of Diamine on the Adhesive Properties*, *ACS Omega.* 9 (2024) 10738–10747.
- [7] P. Patel, R. Patel, J. Chaudhari, R.K. Gupta, *Role of crosslinkers on the properties of bio-based wood adhesives*, *Polym. Eng. Sci.* (2024) Just Accepted (10.1002/pen.26729).
- [8] Z.S. Petrović, X. Wan, O. Bilić, A. Zlatanić, J. Hong, I. Javni, M. Ionescu, J. Milić, D. Degruson, *Polyols and polyurethanes from crude algal oil*, *JAACS, J. Am. Oil Chem. Soc.* 90 (2013) 1073–1078.
- [9] F. M. de Souza, J. Choi, S. Bhoyate, P.K. Kahol, R.K. Gupta, *Expendable Graphite as an Efficient Flame-Retardant for Novel Partial Bio-Based Rigid Polyurethane Foams*, *Carbon Res.* 6 (2020) 27.
- [10] P. Arachchil, A. Perena, R. Gupta, *Preparation of Flame-Retardant Rigid Polyurethane Foams by Combining Modified Melamine– Formaldehyde Resin and Phosphorus Flame Retardants*, (2022).
- [11] S. Bhoyate, M. Ionescu, P.K. Kahol, J. Chen, S.R. Mishra, R.K. Gupta, *Highly flame-retardant polyurethane foam based on reactive phosphorus polyol and limonene-based polyol*, *J. Appl. Polym. Sci.* 135 (2018) 16–19.
- [12] S. Bhoyate, M. Ionescu, P.K. Kahol, R.K. Gupta, *Castor-oil derived nonhalogenated reactive flame-retardant-based polyurethane foams with significant reduced heat release rate*, *J. Appl. Polym. Sci.* 136 (2019) 47276.
- [13] C. Zhang, S. Bhoyate, M. Ionescu, P.K. Kahol, R.K. Gupta, *Highly flame retardant and bio-based rigid polyurethane foams derived from orange peel oil*, *Polym. Eng.*

Sci. 58 (2018) 2078–2087.

- [14] S. Bhoyate, M. Ionescu, D. Radojcic, P.K. Kahol, J. Chen, S.R. Mishra, R.K. Gupta, Highly flame-retardant bio-based polyurethanes using novel reactive polyols, *J. Appl. Polym. Sci.* 135 (2018) 46027.
- [15] R.K. Gupta, M. Ionescu, X. Wan, D. Radojcic, N. Bilic, New polyols with isocyanuric structure by thiol-ene “click” chemistry reactions, *J. Cell. Plast.* 53 (2017) 639–662.
- [16] R. Scaffaro, A. Maio, F. Suter, E. ortunato Gulino, M. Morreale, Degradation and recycling of films based on biodegradable polymers: A short review, *Polymers (Basel)*. 11 (2019).
- [17] X. Shi, T.A. Nguyen, Z. Suo, Y. Liu, R. Avci, Effect of nanoparticles on the anticorrosion and mechanical properties of epoxy coating, *Surf. Coatings Technol.* 204 (2009) 237–245.
- [18] H. Kim, A.L. Yarin, M.W. Lee, Self-healing corrosion protection film for marine environment, *Compos. Part B Eng.* 182 (2020) 107598.
- [19] C.Y. Barlow, D.C. Morgan, Polymer film packaging for food: An environmental assessment, *Resour. Conserv. Recycl.* 78 (2013) 74–80.
- [20] D.S. Bag, S.N. Ghosh, S. Maiti, Surface modification and evaluation of polyethylene film, *Eur. Polym. J.* 34 (1998) 855–861.
- [21] D. Feldman, Polymer history, *Des. Monomers Polym.* 11 (2008) 1–15.
- [22] F.C. Film, Flexible Conductive Film, (2020) 1–14.
- [23] M.P. Carbonell-Blasco, M.A. Moyano, C. Hernández-Fernández, F.J. Sierra-Molero, I.M. Pastor, D.A. Alonso, F. Arán-Aís, E. Orgilés-Calpena, Polyurethane Adhesives with Chemically Debondable Properties via Diels–Alder Bonds, *Polymers (Basel)*. 16 (2024).
- [24] D. Wang, J. Zhao, P. Claesson, P. Christakopoulos, U. Rova, L. Matsakas, E. Ytreberg, L. Granhag, F. Zhang, J. Pan, Y. Shi, A strong enhancement of corrosion and wear resistance of polyurethane-based coating by chemically grafting of organosolv lignin, *Mater. Today Chem.* 35 (2024) 101833.
- [25] F.M. de Souza, P.K. Kahol, R.K. Gupta, Introduction to Polyurethane Chemistry, in: R.K. Gupta, P.K. Kahol (Eds.), *Polyurethane Chem. Renew. Polyols Isocyanates*, American Chemical Society, Washington, D.C., 2021: p. 1.
- [26] A.R. Kakroodi, M. Khazabi, K. Maynard, M. Sain, O.S. Kwon, Soy-based polyurethane spray foam insulations for light weight wall panels and their performances under monotonic and static cyclic shear forces, *Ind. Crops Prod.* 74 (2015) 1–8.
- [27] V. Kanyanta, A. Ivankovic, Mechanical characterisation of polyurethane elastomer for biomedical applications, *J. Mech. Behav. Biomed. Mater.* 3 (2010) 51–62.

- [28] 1. Introduction, *Eur. J. Public Health*. 32 (2022) 1–43.
- [29] R.J. Slocombe, E.E. Hardy, J.H. Saunders, R.L. Jenkins, Phosgene derivatives. The preparation of isocyanates, carbamyl chlorides and cyanuric acid<sup>1</sup>, *J. Am. Chem. Soc.* 72 (1950) 1888–1891.
- [30] N. V Gama, A. Ferreira, A. Barros-Timmons, Polyurethane foams: Past, present, and future, *Materials (Basel)*. 11 (2018) 1841.
- [31] J. Niesiobędzka, J. Datta, Challenges and recent advances in bio-based isocyanate production, *Green Chem.* 25 (2023) 2482–2504.
- [32] D.P. Pfister, Y. Xia, R.C. Larock, Recent advances in vegetable oil-based polyurethanes, *ChemSusChem*. 4 (2011) 703–717.
- [33] T. Vanbésien, E. Monflier, F. Hapiot, Hydroformylation of vegetable oils: More than 50 years of technical innovation, successful research, and development, *Eur. J. Lipid Sci. Technol.* 118 (2016) 26–35.
- [34] Y. Wang, L. Deng, Y. Fan, Preparation of Soy-Based Adhesive Enhanced by Waterborne Polyurethane: Optimization by Response Surface Methodology, *Adv. Mater. Sci. Eng.* 2018 (2018).
- [35] R. Kaur, P. Singh, S. Tanwar, G. Varshney, S. Yadav, Assessment of Bio-Based Polyurethanes: Perspective on Applications and Bio-Degradation, *Macromol.* 2 (2022) 284–314.
- [36] L. Hojabri, X. Kong, S.S. Narine, Fatty Acid-Derived diisocyanate and biobased polyurethane produced from vegetable oil: Synthesis, polymerization, and characterization, *Biomacromolecules*. 10 (2009) 884–891.
- [37] L. Polyols, Lignin-Derived Polyols, Polyisocyanates, and Polyurethanes, (1981).
- [38] A. Cornille, R. Auvergne, O. Figovsky, B. Boutevin, S. Caillol, A perspective approach to sustainable routes for non-isocyanate polyurethanes, Elsevier Ltd, 2017.
- [39] H. Sardon, A. Pascual, D. Mecerreyes, D. Taton, H. Cramail, J.L. Hedrick, Synthesis of Polyurethanes Using Organocatalysis: A Perspective, *Macromolecules*. 48 (2015) 3153–3165.
- [40] I. Javni, D.P. Hong, Z.S. Petrović, Soy-based polyurethanes by nonisocyanate route, *J. Appl. Polym. Sci.* 108 (2008) 3867–3875.
- [41] F. Magliozzi, G. Chollet, E. Grau, H. Cramail, Benefit of the Reactive Extrusion in the Course of Polyhydroxyurethanes Synthesis by Aminolysis of Cyclic Carbonates, *ACS Sustain. Chem. Eng.* 7 (2019) 17282–17292.
- [42] S. Panchireddy, B. Grignard, J.-M. Thomassin, C. Jerome, C. Detrembleur, Catechol Containing Polyhydroxyurethanes as High-Performance Coatings and Adhesives, *ACS Sustain. Chem. Eng.* 6 (2018) 14936–14944.
- [43] S. Panchireddy, B. Grignard, J.-M. Thomassin, C. Jerome, C. Detrembleur, Bio-

- based poly(hydroxyurethane) glues for metal substrates, *Polym. Chem.* 9 (2018) 2650–2659.
- [44] M. Fleischer, H. Blattmann, R. Mülhaupt, Glycerol-, pentaerythritol- and trimethylolpropane-based polyurethanes and their cellulose carbonate composites prepared via the non-isocyanate route with catalytic carbon dioxide fixation, *Green Chem.* 15 (2013) 934–942.
- [45] A. Cornille, Y. Ecochard, M. Blain, B. Boutevin, S. Caillol, Synthesis of hybrid polyhydroxyurethanes by Michael addition, *Eur. Polym. J.* 96 (2017) 370–382.
- [46] O. Türünç, N. Kayaman-Apohan, M.V. Kahraman, Y. Menciloğlu, A. Güngör, Nonisocyanate based polyurethane/silica nanocomposites and their coating performance, *J. Sol-Gel Sci. Technol.* 47 (2008) 290–299.
- [47] H.J. Assumption, L.J. Mathias, Photopolymerization of urethane dimethacrylates synthesized via a non-isocyanate route, *Polymer (Guildf)*. 44 (2003) 5131–5136.
- [48] O.L. Figovsky, L.D. Shapovalov, Features of reaction amino-cyclocarbonate for production of new type nonisocyanate polyurethane coatings, *Macromol. Symp.* 187 (2002) 325–332.
- [49] C. Wang, Z. Wu, L. Tang, J. Qu, Synthesis and properties of cyclic carbonates and non-isocyanate polyurethanes under atmospheric pressure, *Prog. Org. Coatings*. 127 (2019) 359–365.
- [50] A. Steblyanko, W. Choi, F. Sanda, T. Endo, Addition of five-membered cyclic carbonate with amine and its application to polymer synthesis, *J. Polym. Sci. Part A Polym. Chem.* 38 (2000) 2375–2380.
- [51] S. Takahashi, Lactate and Ketone Bodies Act as Energy Substrates as Well as Signal Molecules in the Brain, *Psychol. Pathophysiol. Outcomes Eat.* (2021).
- [52] N. Dhore, E. Prasad, R. Narayan, C.R.K. Rao, A. Palanisamy, Studies on Biobased Non-Isocyanate Polyurethane Coatings with Potential Corrosion Resistance, *Sustain. Chem.* 4 (2023) 95–109.
- [53] S. Doley, S.K. Dolui, Solvent and catalyst-free synthesis of sunflower oil based polyurethane through non-isocyanate route and its coatings properties, *Eur. Polym. J.* 102 (2018) 161–168.
- [54] A.-S. Mora, R. Tayouo, B. Boutevin, G. David, S. Caillol, A perspective approach on the amine reactivity and the hydrogen bonds effect on epoxy-amine systems, *Eur. Polym. J.* 123 (2020) 109460.
- [55] M. Bähr, A. Bitto, R. Mülhaupt, Cyclic limonene dicarbonate as a new monomer for non-isocyanate oligo- and polyurethanes (NIPU) based upon terpenes, *Green Chem.* 14 (2012) 1447–1454.
- [56] B. Tamami, S. Sohn, G.L. Wilkes, Incorporation of carbon dioxide into soybean oil and subsequent preparation and studies of nonisocyanate polyurethane networks, *J. Appl. Polym. Sci.* 92 (2004) 883–891.

- [57] A. Asefnejad, M.T. Khorasani, A. Behnamghader, B. Farsadzadeh, S. Bonakdar, Manufacturing of biodegradable polyurethane scaffolds based on polycaprolactone using a phase separation method: physical properties and in vitro assay, *Int. J. Nanomedicine*. (2011) 2375–2384.
- [58] R.C.M. Dias, A.M. Góes, R. Serakides, E. Ayres, R.L. Oréface, Porous biodegradable polyurethane nanocomposites: preparation, characterization, and biocompatibility tests, *Mater. Res.* 13 (2010) 211–218.
- [59] A.N.F. Mendes, J.R. Gregório, R.G. da Rosa, Studies on the experimental variables effects on rhodium catalyzed hydroformylation of unsaturated fatty esters and comparison of  $[\text{RhH}(\text{CO})(\text{PPh}_3)_3]$  and  $[\text{RhCl}_3 \cdot 3\text{H}_2\text{O}]$  as starting catalytic precursors, *J. Braz. Chem. Soc.* 16 (2005) 1124–1129.
- [60] W. Liu, G. Lu, B. Xiao, C. Xie, Potassium iodide–polyethylene glycol catalyzed cycloaddition reaction of epoxidized soybean oil fatty acid methyl esters with  $\text{CO}_2$ , *RSC Adv.* 8 (2018) 30860–30867.
- [61] X. He, X. Xu, Q. Wan, G. Bo, Y. Yan, Solvent- and Catalyst-free Synthesis, Hybridization and Characterization of Biobased Nonisocyanate Polyurethane (NIPU), *Polymers (Basel)*. 11 (2019).
- [62] O. Mó, M. Yáñez, M. Eckert-Maksić, Z.B. Maksić, I. Alkorta, J. Elguero, Periodic Trends in Bond Dissociation Energies. A Theoretical Study, *J. Phys. Chem. A*. 109 (2005) 4359–4365.
- [63] H. Wu, B. Jin, H. Wang, W. Wu, Z. Cao, J. Wu, G. Huang, A Degradable and Self-Healable Vitriimer Based on Non-isocyanate Polyurethane, *Front. Chem.* 8 (2020).
- [64] A. Lee, Y. Deng, Green polyurethane from lignin and soybean oil through non-isocyanate reactions, *Eur. Polym. J.* 63 (2015) 67–73.
- [65] G. Beniah, D.J. Fortman, W.H. Heath, W.R. Dichtel, J.M. Torkelson, Non-Isocyanate Polyurethane Thermoplastic Elastomer: Amide-Based Chain Extender Yields Enhanced Nanophase Separation and Properties in Polyhydroxyurethane, *Macromolecules*. 50 (2017) 4425–4434.
- [66] J. Ke, X. Li, S. Jiang, C. Liang, J. Wang, M. Kang, Q. Li, Y. Zhao, Promising approaches to improve the performances of hybrid non-isocyanate polyurethane, *Polym. Int.* 68 (2019) 651–660.